

SEARCHING FOR NEW GENES THAT CAUSE USHER SYNDROME

Ala Moshiri , Niusha Kasiri , Michael Shea , Layla Ali , Benjamin Yang , Andy Shao , Dave Clary , Ann M. Flenniken , Mohammad Eskandarian , Oana V. Amarie , Lore Becker , Riccardo Sangermano , Emily M. Place , Kinga M. Bujakowska , Rachel M. Huckfeldt , Zorana Berberovic , Raphaël Bour , Fabrice Riet , Steve D. Brown , Abigail D'Souza , Helmut Fuchs , Valerie Gailus-Durner , Alain Guimond , Yann Hérault , Martin Hrabec de Angelis , Aline Lux , Christophe Mittelhauser , Lauryl M.J. Nutter , Marcela Palkova , Jiri Lindovsky , Benoit Petit-Demouliere , Jan Prochazka , Vivian Bradaschia , Lois Kelsey , Colin McKerlie , Miles Joseph Raishbrook , Radislav Sedlacek , The International Mouse Phenotyping Consortium, Louise Lanoue , KC Kent Lloyd , Michel J. Roux , Olivia Bermingham-McDonogh

PII: S0002-9394(26)00323-5
DOI: <https://doi.org/10.1016/j.ajo.2026.06.016>
Reference: AJOPHT 13993

To appear in: *American Journal of Ophthalmology*

Received date: January 21, 2026
Accepted date: June 8, 2026

Please cite this article as: Ala Moshiri , Niusha Kasiri , Michael Shea , Layla Ali , Benjamin Yang , Andy Shao , Dave Clary , Ann M. Flenniken , Mohammad Eskandarian , Oana V. Amarie , Lore Becker , Riccardo Sangermano , Emily M. Place , Kinga M. Bujakowska , Rachel M. Huckfeldt , Zorana Berberovic , Raphaël Bour , Fabrice Riet , Steve D. Brown , Abigail D'Souza , Helmut Fuchs , Valerie Gailus-Durner , Alain Guimond , Yann Hérault , Martin Hrabec de Angelis , Aline Lux , Christophe Mittelhauser , Lauryl M.J. Nutter , Marcela Palkova , Jiri Lindovsky , Benoit Petit-Demouliere , Jan Prochazka , Vivian Bradaschia , Lois Kelsey , Colin McKerlie , Miles Joseph Raishbrook , Radislav Sedlacek , The International Mouse Phenotyping Consortium, Louise Lanoue , KC Kent Lloyd , Michel J. Roux , Olivia Bermingham-McDonogh , SEARCHING FOR NEW GENES THAT CAUSE USHER SYNDROME, *American Journal of Ophthalmology* (2026), doi: <https://doi.org/10.1016/j.ajo.2026.06.016>



This is a PDF of an article that has undergone enhancements after acceptance, such as the addition of a cover page and metadata, and formatting for readability. This version will undergo additional copyediting, typesetting and review before it is published in its final form. As such, this version is no longer the Accepted Manuscript, but it is not yet the definitive Version of Record; we are providing this early version to give early visibility of the article. Please note that Elsevier's sharing policy for the Published Journal Article applies to this version, see: <https://www.elsevier.com/about/>

[policies-and-standards/sharing#4-published-journal-article](#). Please also note that, during the production process, errors may be discovered which could affect the content, and all legal disclaimers that apply to the journal pertain.

© 2026 Published by Elsevier Inc.

SEARCHING FOR NEW GENES THAT CAUSE USHER SYNDROME

Ala Moshiri, MD, PhD^{1#}, Niusha Kasiri, MD^{1#}, Michael Shea, BS¹, Layla Ali, BA², Benjamin Yang, MD¹, Andy Shao, MD¹, Dave Clary, BS³, Ann M. Flenniken, PhD^{4,5}, Mohammad Eskandarian^{4,5}, Oana V. Amarie, PhD⁶, Lore Becker⁶, Riccardo Sangermano, PhD⁷, Emily M. Place, MS⁷, Kinga M. Bujakowska, PhD⁷, Rachel M. Huckfeldt, MD, PhD⁷, Zorana Berberovic^{4,5}, Raphaël Bour⁸, Fabrice Riet⁸, Steve D. Brown, PhD⁹, Abigail D'Souza, MSc^{4,5}, Helmut Fuchs, PhD⁶, Valerie Gailus-Durner, PhD⁶, Alain Guimond⁸, Yann Hérault, PhD^{8,17}, Martin Hrabe de Angelis, PhD^{6,10,11}, Aline Lux, BTS⁸, Christophe Mittelhauser⁸, Lauryl M. J. Nutter, PhD^{4,12}, Marcela Palkova, PhD¹³, Jiri Lindovsky, PhD¹³, Benoit Petit-Demouliere, PhD⁸, Jan Prochazka, PhD¹³, Vivian Bradaschia, PhD^{4,5}, Lois Kelsey^{4,5}, Colin McKerlie, DVM, DVSc^{14,15}, Miles Joseph Raishbrook, MSc¹³, Radislav Sedlacek, PhD¹³, The International Mouse Phenotyping Consortium⁸, Louise Lanoue, PhD³, KC Kent Lloyd, DVM, PhD^{3,16}, Michel J. Roux, PhD¹⁷, Olivia Bermingham-McDonogh, PhD¹⁸

Institutional Affiliations:

¹Department of Ophthalmology & Vision Science, School of Medicine, University of California-Davis, Davis, California, United States.

²College of Medicine, California Northstate University, 9700 W Taron Dr, Elk Grove, CA 95757, USA.

³Mouse Biology Program, University of California-Davis, Davis, California, United States.

⁴The Centre for Phenogenomics, The Hospital for Sick Children, Toronto, ON, Canada.

⁵Lunenfeld-Tanenbaum Research Institute, Mount Sinai Hospital, Toronto, ON, M5G 1X5, Canada.

⁶Institute of Experimental Genetics and German Mouse Clinic, Helmholtz Munich, Neuherberg, Germany.

⁷Ocular Genomics Institute, Massachusetts Eye and Ear, Department of Ophthalmology, Harvard Medical School, Boston, MA, USA.

⁸Université de Strasbourg, CNRS UMR 7104, INSERM U 1258, IGBMC, Institut Clinique de la Souris, PHENOMIN, Illkirch-Graffenstaden, France.

⁹Medical Research Council, Harwell Institute, Harwell, UK.

¹⁰German Center for Diabetes Research (DZD), Neuherberg, Germany.

¹¹Chair of Experimental Genetics, TUM School of Life Sciences, Technische Universität München, Freising, Germany.

¹²Program in Genetics and Genome Biology, The Hospital for Sick Children, Toronto, ON, M5G 1 X8, Canada.

¹³Czech Centre for Phenogenomics, Institute of Molecular Genetics of the Czech Academy of Sciences, Vestec, Czech Republic.

¹⁴Translational Medicine, The Hospital for Sick Children, Toronto, ON, Canada.

¹⁵Department of Laboratory Medicine & Pathobiology, Faculty of Medicine, University of Toronto, Toronto, ON, Canada.

¹⁶Department of Surgery, School of Medicine, University of California Davis, Sacramento, CA, United States.

¹⁷Institut de Génétique et de Biologie Moléculaire et Cellulaire, Université de Strasbourg, Illkirch, France.

¹⁸Department of Neurobiology and Biophysics, University of Washington School of Medicine, Seattle, WA 98195, USA.

#These authors contributed equally to this work.

*Corresponding author:

Ala Moshiri MD, PhD

Department of Ophthalmology and Vision Science, School of Medicine

UC Davis Eye Center

Ernest E. Tschannen Eye Institute

4860 Y. Street, Suite 2400

Sacramento, CA 95817

Phone: (916) 734-6602

Fax: (916) 734-6197

Email: amoshiri@health.ucdavis.edu

ABSTRACT

PURPOSE: The purpose of this project was to identify novel Usher syndrome (USH) candidate genes from phenotyping data of 9,139 knockout (KO) mouse lines.

METHODS: We evaluated phenotype data for concurrent retinopathy and hearing abnormalities in single-gene KO mice generated by the International Mouse Phenotyping Consortium (IMPC). A search was performed to determine if each gene had been previously established in retinopathy and/or deafness in humans. Bioinformatic tools were used to predict protein interactions, molecular functions, signaling pathways, and expression of human orthologs of candidate genes in retina and inner ear.

RESULTS: We identified 18 single-gene KO lines exhibiting hearing abnormality and retinopathy after ear and eye examination, respectively, and/or by histopathology. The molecular functions and signaling pathways of the human orthologues of 18 candidate genes partially overlapped with USH genes. Particularly, FER and DYRK1B proteins were predicted to interact with proteins encoded by known ciliopathy genes. *ADIPOR1*, *ATP8B1* and *MPDZ* were associated with retinal degeneration in humans. *CHSY1* and *IDUA* may be a pathogenic cause of hearing impairment in people. Additionally, *CHSY1*, *CSTB* and *SPRED1* were located adjacent to unsolved genetic loci related to USH.

CONCLUSIONS: A screen of 9,139 KO mouse lines revealed 18 candidate genes exhibiting both retinal and inner ear abnormality consistent with principle clinical features associated with USH. As the observed phenotypes are attributed to gene deletion in mice, these genes warrant further study to determine causation of retinal degeneration and hearing loss in patients.

KEYWORDS: Usher syndrome, Retinal abnormality, Auditory abnormality, Dual sensory impairment, Knockout mouse, genetic variants

INTRODUCTION

The combination of vision and hearing loss, referred to as dual sensory impairment (DSI), can be caused by widely different conditions and affect 11.3% of the United States population aged 80 and older.¹ Congenital forms of DSI are often heritable single gene disorders such as Usher syndrome (USH), Bardet-Biedel syndrome (BBS), Stickler syndrome, Waardenburg syndrome, Alstrom disease, Tietz albinism-deafness syndrome, Norrie disease, Charge syndrome, Alport syndrome, and mitochondrial DNA disorders like Kearns-Sayre syndrome and maternally-inherited diabetes and deafness.² USH has a prevalence of 1-4 in 25,000 individuals, and is the most common DSI phenotype.³

USH is an autosomal recessive (AR) condition affecting the photoreceptors in the retina as well as the hair cells (HCs) of the cochlea and vestibule in the inner ear, resulting in retinitis pigmentosa (RP), sensorineural hearing loss (SNHL) and variable vestibular dysfunction.⁴ Symptoms and signs of USH have different severities and onsets, categorized into four main clinical types (USH1, USH2, USH3, USH4).² Pathogenic variants in ten different genes are associated with USH: *MYO7A*, *USH1C*, *CDH23*, *PCDH15* and *USH1G* for USH1; *USH2A*, *ADGRV1* and *WHRN* for USH2; *CLRN1* for USH3 and *ARSG* for USH4.² The association of five additional genes (*ABHD12*, *CEP250*, *CEP78*, *ESPN* and *PDZD7*) related to this syndrome remains unclear.^{2,5,6} Further, there are likely additional genes at three genomic loci mapped to USH1: 10p11.21-q21.1, 15q22-q23, and 21q21,^{2,6} confirming that unknown USH genes could exist.

Structural USH proteins in the inner ear are organized into major complexes that are essential for the function and stability of sensory hair cells, which convert sound vibrations into neuronal signals. Usher protein complex 1 (encoded by *MYO7A*, *USH1C*, *USH1G*, *PCDH15* and *CDH23*) is localized at the tip links and lateral links of hair cell stereocilia, specialized structures that mediate mechano-electrical transduction. Disruption of this complex compromises the physical coupling between stereocilia, leading to defective sound and balance perception. Usher protein complex 2 (encoded by *USH2A*, *ADGRV1*, *WHRN*, and *PDZD7*) is found at the ankle links, which provide structural support and maintain proper stereocilia organization. In the retina, components of Usher protein complex 1 are localized at membrane interfaces between the calyceal processes and the basolateral region of the outer segment in both rods and cones, as well as the junction between the inner and outer segments in rod photoreceptors. These regions are critical for maintaining the structural stability and alignment of the photoreceptor outer segments. In contrast, Usher protein complex 2 is concentrated at the periciliary region of photoreceptors, where it supports the organization and trafficking of proteins essential for photoreceptor maintenance and function.⁷

Several animal models have been used to study the underlying process of USH and to establish potential therapies.⁵ Historically, mice have served as USH models, but only partly recapitulating the retinal phenotype,

which is generally milder in rodents.^{5,8} This discordance with the human phenotype is attributed to mouse photoreceptors lacking human-like calyceal processes and periciliary membranes.⁵ However, due to the existence of not-yet-discovered USH genes in humans, evident by unsolved genomic loci, we employed knockout (KO) mouse lines to search for novel candidates, despite these species differences. These candidate genes may highlight new molecular mechanisms underlying the pathobiology of USH and help identify new genotype-phenotype associations.

METHODS AND MATERIALS

IMPC KNOCKOUT MOUSE LINES

The IMPC⁹⁻¹⁵ (<https://www.mousephenotype.org/>) consists of 13 phenotyping centers worldwide, aiming to generate and phenotype single-gene KO mouse lines for all coding genes in the mouse genome. Phenotyping data of each line is gathered using a set of tests from the International Mouse Phenotyping Resource of Standardised Screens (IMPreSS, <https://www.mousephenotype.org/impress/index>).⁹ All lines were generated and maintained on a C57BL/6N genetic background.¹⁰ The technology adopted for generating each single-gene KO line was initially publicly available targeted mouse embryonic stem (ES) cells,¹¹ then replaced by Cas9-mediated deletion strategies in 2014.¹² For each gene, the Consortium produced and phenotyped seven males and seven females for most tests as defined in IMPreSS. For gene KOs affecting viability, with subviability defined as <12.5% live homozygotes (HOM) from heterozygote (HET) crosses, HET mice were phenotyped. KO and corresponding age and sex-matched wild-type (WT) control mice were phenotyped as young adults between 9 and 16 weeks of age. At 14 weeks, hearing ability for at least four mutant mice, both males and females in most cases, was evaluated by analyzing auditory brainstem response (ABR) at frequencies of 6, 12, 18, 24 and 30 kHz. A click-evoked ABR was optional.¹³ Complete ophthalmic examination was performed at week 15 or 16. For primary screen of the retinal traits, almost all phenotyping centers used slit lamp examination (except for Baylor College of Medicine and HMGU Helmholtz Munich) and indirect fundus examination (except for Baylor College of Medicine, HMGU Helmholtz Munich, and Institut Clinique de la Souris — PHENOMIN-ICS, which instead conducted routine optical coherence tomography (OCT) cross-sectional and funduscopy imaging) as the primary screen tools. Hematoxylin and eosin staining on formalin-fixed paraffin-embedded tissues was additionally used by The Center for Phenogenomics and University of California Davis. Depending on the applied test and/or instrumentation used, the secondary screen studies varied across the phenotyping centers, and included electroretinogram (ERG), OCT, fundus imaging, and transmission electron microscopy (TEM).¹⁴ Phenotyping data obtained from HET or HOM mice were compared to WT control mice from the same center with genotypes masked to the evaluators. If the phenotypic difference was statistically significant,¹⁵ an ontology term from the Mammalian Phenotype ontology was used to describe the phenotype.⁹

The IMPC guidelines related to housing and husbandry met the requirements of the ARRIVE guidelines,¹⁶ the Gold Standard publication Checklist reporting Guidelines, and the Genetically Altered (GA) Passport to maintain animal welfare. All procedures complied with local, state, and national regulatory guidelines and have been reviewed and approved by associated institutional animal care and use committees (IACUC), animal care committees (ACC), or equivalent.

NOVEL CANDIDATE GENES IDENTIFIED

The IMPC KO mouse lines⁹⁻¹⁵ database (version 23, released on April 23, 2025) was queried for 11 retinal and 2 auditory traits. Retinal traits included abnormal retina morphology, retina pigmentation, eye electrophysiology, outer nuclear layer morphology, blood vessel morphology, vasculature morphology, blood vessel pattern, inner nuclear layer morphology, optic vesicle formation, decreased and increased total retina thickness, while auditory traits were abnormal auditory brainstem response (ABR) and abnormal otic vesicle morphology.

To identify potential candidate genes for USH that are not part of the 16 genes mentioned previously, the genes correlated with hearing and retina abnormality were screened for the ones that showed at least one retinal and one auditory trait, concurrently. To increase the stringency of assessment of causation of disease, only the candidate genes causing bilateral retinopathy in the majority of mice (a minimum of half of the KO mice in males and/or females affected) and/or were validated by histopathology were included. Mouse lines with retinal findings that did not meet these additional criteria were excluded despite achieving statistical significance by IMPC standards.

SUBSTITUTION OF MOUSE GENES WITH HUMAN ORTHOLOGUES

We used the GeneCards database (<https://www.genecards.org>) v5.25 (updated: July 23, 2025)^{17,18} to search for human orthologues of the candidate mouse genes for multiple analyses including protein interactions, molecular functions, and signaling pathways. Additionally, mouse orthologues of inherited DSI genes were used to assess whether mouse lines with those genes disrupted recapitulate any DSI phenotypes. By employing this database, we also screened the locus of the human orthologue of each candidate gene to see if any were positioned in proximity of any of the previously mentioned three known mapped USH loci.

PROTEIN-PROTEIN INTERACTION NETWORK

A protein interaction analysis was performed between the proteins encoded by USH genes, other established inherited DSI genes, ciliopathy genes, and our candidate genes by STRING-db v12.0 released 26th July 2023¹⁹ built in Cytoscape 3.10.3 App, StringApp.²⁰ A confidence threshold of 0.9 was used to visualize any interaction between the proteins encoded by members of each group. To delve deeper into possible interactions among the four gene sets, an analysis with the confidence level of 0.7 was also performed.

MOLECULAR FUNCTIONS AND SIGNALING PATHWAYS

An analysis based on v19.0 of the PANTHER classification system, released June 20, 2024 (<https://www.pantherdb.org/>) was conducted to investigate the molecular functions contributed by each gene group.^{21,22} Associated signaling pathways were analyzed by KEGG, Reactome, and WIKI pathways through The Database for Annotation, Visualization, and Integrated Discovery (DAVID) knowledgebase v2025_1, released April 17th 2025 (<https://davidbioinformatics.nih.gov/>).^{23,24}

ASSESSMENT OF GENE EXPRESSION IN RETINA AND INNER EAR

Gene expression in the retina was analyzed using the expression plot of PPlatform for Analysis of scEiad (single cell eye in a disk) or Plae v0.95 (<https://plae.nei.nih.gov/>).²⁵ We used the “CellType_predict” cell grouping and set the facet on “Gene”, in addition to “organism” and “CellType_predict” as filter category in a minimum of 50 cells per group to narrow our analysis to include the data from *Homo sapiens* and *Mus musculus* separately. As RP in USH predominantly affects rod photoreceptors and/or retinal pigment epithelium (RPE) cells,⁶ we checked the expression of the candidate genes and USH genes only in these cells, based on “Mean Log2(Counts+1)” values which were colored based on “study_accession”. Consequently, if the presented value for RPE cells and/or rod photoreceptors was greater than zero, then the gene was considered expressed in the retina. For values equal to zero the expression was considered as not detected. Similarly, we used the Gene Expression Analysis Resource (gEAR)²⁶ portal v2 (<https://umgear.org/>) to analyze the expression of each candidate and USH gene in cochlea and/or vestibular HCs of humans and mice. Expression of the gene in either cochlea or vestibular HCs was considered as the expression of the gene in the inner ear. Human Inner Ear and Inner Ear Organoid (van der Valk and coworkers, 2023²⁷) profile was used for detection of gene expression in humans. In this profile, single nucleus RNA-sequencing (snRNA-seq) of inner ear HCs at fetal age weeks 7.5 and 9.2 exhibit the transcription of each gene in vestibular HCs, as the mature cochlea is still in development.²⁷ The single cell RNA sequencing (scRNA-seq) data of vestibular and inner hair cells/outer hair cells (IHC/OHC) demo profiles were used to identify the expression of candidates in the utricle and cochlear HCs of mice, respectively.

ASSOCIATION WITH RETINAL DISORDERS AND DEAFNESS

We used the retinal information network (RetNet, <https://retnet.org/>), accessed on September 5th, 2025, to find any known association of human orthologues of candidate genes with retinopathies or mapped loci associated with retinopathies.²⁸ Also, we carried out a similar study for hearing impairment by using the shared Harvard inner-ear laboratory database (SHIELD, <https://shield.hms.harvard.edu/>),²⁹ accessed on September 5th, 2025, and the deafness variation database (DVD, <https://deafnessvariationdatabase.org/>) v9.2, accessed: September 30, 2025.³⁰ In DVD, we searched through the variant table of each represented gene using the value of hearing impairment in the phenotype field. The 263 genes related to ciliopathies, a combination of Syscilia and Ciliacarta, and 39 genes of other inherited DSI illnesses were derived from Higgins and coworkers, 2022³¹ and Guimaraes and colleagues, 2023,² respectively. Additionally, previously established associations of the candidate genes with retinal, hearing, and other clinical phenotypes in humans were retrieved from Online Mendelian Inheritance in Man, OMIM®.

McKusick-Nathans Institute of Genetic Medicine, Johns Hopkins University (Baltimore, MD), <https://omim.org/>, accessed in September 2025.

LITERATURE REVIEW ON KO MOUSE LINES

To investigate the retinal and auditory phenotype of variant mouse lines in greater detail, we performed a literature search on KO and/or HET mouse lines for each candidate and mouse orthologue of inherited DSI genes, which were generated and studied for inner ear and retinal abnormalities. The auditory and retinal phenotype of lines were individually investigated (<https://pubmed.ncbi.nlm.nih.gov/> and <https://scholar.google.com/>) by searching “gene symbol”, “knockout” or “deletion” or “null”, “mouse”, “ear”, “retina”, “hearing” and “eye” terms to make associations between the genes and previously mentioned abnormal traits.

ETHICS STATEMENT

The study was approved by the institutional review board of Partners HealthCare System and adhered to the Declaration of Helsinki. Informed consent was obtained from all individuals on whom genetic testing and further molecular evaluations were performed.

CLINICAL EVALUATION

Patients and available family members from 230 families with syndromic or non-syndromic IRD were ascertained at Massachusetts Eye and Ear, enrolled in a study assessing elusive causality. Clinical evaluation was performed by experienced ophthalmologists according to previously published protocols and included functional and structural assessment.³²⁻³⁵

GENETIC ANALYSIS

Blood samples were obtained from probands and, when possible, their family members. DNA was isolated from peripheral blood lymphocytes by standard procedures. Genome sequencing was performed at Massachusetts Eye and Ear, and data were aligned to hg38, and variant calling was performed using DRAGEN-GATK4 best practice. GATK-structural variant (SV) cohort mode using five different algorithms was used for structural variant calling.³⁶

STATISTICAL ANALYSIS

Statistical analysis was done by using GraphPad Prism version 10.5.0. ERG data were presented as mean \pm SD. Due to different variances among the groups (53 WT vs four *Mpdz*^{-/-} and three *Rnf10*^{-/-} mice), Welch’s t test was used to compare the ERG wave amplitudes. A $p < .05$ was considered statistically significant. For OCT data, presented as mean \pm SD, retinal thickness was compared between *Idua*^{-/-} and WT mice using the Wilcoxon rank-sum test, with significance defined as $p < .05$. The ABR test results in KO lines, conducted by IMPC, with p -values equal or lower to 10^{-4} ($p \leq .0001$) were marked as significant.

RESULTS

IDENTIFICATION OF CANDIDATE HUMAN USH GENES

We queried KO mouse lines phenotyped by the IMPC for retinopathy and hearing abnormalities. We found 813 genes with at least one of 11 distinct abnormal retinal phenotypes and 338 genes with at least one of two distinct ear abnormalities. Fifty genes were identified that caused both auditory and retinal abnormalities in the same mouse line (Fig. 1A). Among these, 18 genes were considered high likelihood candidates for USH as the resultant retinopathy was either confirmed by histopathology and/or was documented with bilaterally symmetric retinal abnormalities in the majority of males and/or females of each mutant mouse line: *AA986860* (MMRRC:066881-UCD), *Adipor1* (EM:08491), *Ankrd11* (retina phenotype: EM:00380, Ear phenotype: EM:07651), *Atp8b1* (MMRRC:067151-UCD), *Chsy1* (MMRRC:067396-UCD), *Cstb* (EM:09566), *Dyrk1b* (EM:10419), *Eef1d* (MMRRC:066978-UCD), *Fer* (MMRRC:066693-UCD), *Idua* (EM:15473), *Mpdz* (MMRRC:048630-UCD), *Pigq* (MMRRC_043931-UCD), *Rnf10* (retina phenotype: MMRRC:049477-UCD and MMRRC_049478-UCD, ear phenotype: MMRRC:049477-UCD), *Slc20a2* (retina phenotype: EM:08067, ear phenotype: EM:05549), *Spred1* (EM:12627), *Sun1* (EM:09532), *Tmem145* (MMRRC:065589-UCD), and *Xrcc5* (EM:12867).⁹⁻¹⁵ Interestingly, genes

like *Ankrd11*, *Dyrk1b*, *Eef1d*, *Slc20a2*, induced relevant USH phenotypes in heterozygous individuals, whereas for the other genes, these phenotypes were only observed in homozygous mutants. The situation for homozygous mutant genes is comparable to the autosomal recessive inheritance of the USHER syndrome mutations while the others may correspond in human to combination of partial loss-of-function. These 18 new genes which are not part of the USH gene list, were considered candidate genes for human USH. Human orthologs for 11 of these genes (*SPRED1*, *PIGQ*, *IDUA*, *ANKRD11*, *ATP8B1*, *CHSY1*, *MPDZ*, *EEF1D*, *CSTB*, *DYRK1B*, *SLC20A2*) were associated with other clinical phenotypes in humans (Supplementary table 1).

In addition to hearing abnormality (Supplementary Fig.1) and retinopathy, many of these 18 mutant lines showed abnormalities in other physiological systems as well, resulting in expansion of the focus of our study to other inherited forms of DSI.² If a particular mutant mouse line affected all the physiologic systems similar to a known form of a human DSI syndrome, that gene was considered to be a candidate for the associated DSI disease. Some mouse lines reported here had significant but not complete similarity with DSI syndromes. As a result, the mutant lines which manifested phenotypes in at least two physiological systems in addition to visual and auditory systems were also considered positive hits for these DSI disorders, as summarized in table 1 (all phenotyping data is available on supplementary data sheet 1).

ACCURACY OF MOUSE LINES IN REPLICATING HUMAN DSI PHENOTYPES

We wished to determine if any of the 18 candidate genes had published mouse models with retinal or hearing phenotypes. Our literature search found that published papers from independent labs showed that all six candidate genes which were studied for retinopathy in KO mice (*Adipor1*,³⁷ *Chsy1*,³⁸ *Idua*,³⁹ *Rnf10*,⁴⁰ *Sun1*,⁴¹ and *Xrcc5*⁴²) showed retinal abnormalities, and that all four candidate genes studied for inner ear abnormalities in KO mice (*Atp8b1*,⁴³ *Idua*,⁴⁴ *Mpdz*,⁴⁵ and *Sun1*⁴⁶) showed the respective abnormalities. We did not find reports of negative retinal or hearing phenotypes in any KO mouse models of the 18 candidate genes.

Furthermore, we wished to assess the degree to which mouse models of USH genes and other established inherited DSI syndromes recapitulate the spectrum of findings seen in humans. To this end, we queried the literature for reports of KO mouse models of 15 human USH genes (ten confirmed genes and five known human candidates).^{2,6} We also queried the IMPC database for any retinal and/or auditory abnormality using the same set of 15 USH genes (Table 2A). The IMPC data studied the retinal phenotype in only nine KO and/or HET mouse lines among the 15 USH genes: *Adgrv1*, *Arsg*, *Cep250*, *Cep78*, *Cln1*, *Espn*, *Myo7a*, *Ush1c*, and *Whrn*. The other 6 genes were either not tested, or the study was not fully analyzed. The IMPC also studied the hearing phenotype of four KO mouse lines out of 15 USH genes: *Adgrv1*, *Cep250*, *Cep78*, and *Cln1*. Only these four lines had complete phenotyping of the eye and ear. The other 11 genes were not tested for hearing, or the results of the tests were not analyzed. Three of the four had abnormal ABR results. None of the 9 lines with ocular phenotyping data had retinopathy.

Analysis of peer-reviewed articles for mouse models of the same 15 human USH genes showed that 14 of the 15 had positive hearing abnormalities. Only 13 of 15 mouse models had published evaluation of the retina, and 9 of the 13 had a retinal phenotype while 4 of 13 had a normal retina.

To compare IMPC screening to independent labs in a head-to-head comparison, we found just four genes that had retinal and hearing evaluations reported by both screening paradigms. Four genes (*Adgrv1*, *Cep250*, *Cep78*, and *Cln1*) had mouse models that were studied for both retinal and inner ear phenotypes by independent labs, showing concurrent retina and inner ear abnormality in three out of four lines (*Cep250*, *Cep78*, and *Cln1*). The IMPC screening of these four lines showed no retinopathy in any of them, but ear abnormalities in three of four (*Adgrv1*, *Cep250*, *Cln1*). The results suggest that longitudinal study of mouse models of USH (as in the published literature) is more sensitive than the high-throughput snapshot screening used by the IMPC. We also concluded that mouse models of USH, when studied longitudinally, recapitulated the human findings associated with hearing (14/15, 93.3%), but the retinal abnormalities were not modeled as faithfully (9/13, 69.2%). All data are shown in Table 2A.

A similar analysis was performed on mouse lines for the other (non-USH) inherited DSI confirmed genes (Table 2B). There were 39 known DSI genes exclusive of USH.² The IMPC has generated and phenotyped the retina of KO/HET/hemizygous mice for 22 out of 39 confirmed DSI genes: *Alms1*, *Bbip1*, *Bbs1*, *Bbs4*, *Bbs5*, *Bbs7*, *Bbs9*, *Bbs10*, *Bbs12*, *Cep290*, *Cfap418*, *Chd7*, *Col11a1*, *Col2a1*, *Col4a3*, *Col4a4*, *Col4a5*, *Col9a2*, *Ifi172*, *Ifi74*, *Mks1*, and *Snai2*. Two of these 22 lines had retinal phenotypes (*Bbs5* and *Ifi72*, 9.1%). The IMPC has also reported on the hearing ability of 14 KO/HET/hemizygous mouse lines out of 39 DSI genes: *Alms1*, *Bbs1*, *Bbs4*, *Bbs7*, *Bbs10*,

Cep290, *Cfap418*, *Col4a3*, *Col4a4*, *Col4a5*, *Col9a2*, *Ift172*, *Ift74*, and *Snai2*. Just *Col9a2* (1/14, 7.1%) had abnormal hearing.

Independent publications evaluated mouse models in 20 of 39 DSI genes for retinal abnormalities and found phenotypes in 17 of them (17/20, 85%). Independent labs evaluated hearing for 16 DSI genes using mouse models, all of which were abnormal (16/16, 100%).

We then performed a head-to-head comparison for DSI mouse models between IMPC high-throughput snapshot screening versus longitudinal evaluation by independent research labs. Eleven lines were analyzed by both paradigms for retinal phenotypes and 6 lines were analyzed by both methods for hearing. Only two lines were characterized for both inner ear and retinal phenotypes by both strategies. Results are outlined in Table 3.

Taken together, these data suggest that mouse models of USH and other DSI syndromes recapitulate the human findings when studied longitudinally as in the case of peer-reviewed articles from independent research labs. However, the IMPC high-throughput phenotyping pipeline was relatively less sensitive (but specific) for picking up these abnormalities. This could be due to the nature of high-throughput screening, so only the most prominent phenotypes are recorded. In contrast, individual research projects looking at specific genes are more focused and conduct deeper phenotyping.

ANALYZING THE EXPRESSION OF USHER GENES AND CANDIDATE GENES IN THE RETINA AND INNER EAR

Fifteen human USH genes and 18 candidate genes were analyzed for retinal expression (rods and/or RPE cells) and inner ear cells (cochlear and/or vestibular HCs) of humans and mice, cells that are primarily affected in RP and/or SNHL, as seen in USH.⁶

We screened the Plae database²⁵ to study the expression of the two gene sets in the rods and/or RPE cells of the retina of both species. We found that 13/15 (86.6%) of human USH genes are expressed in the retina of humans and mice. The expression of *CLRN1* and *USH1G* was not detected in the human rods and/or RPE cells. Mouse rods and/or RPE cells showed no transcripts of *Ush1g* and *Pdzd7*. In terms of our candidate genes, 16/18 (88.8%) and 17/18 (94.4%) are expressed in the retina of humans and mice, respectively. No expression of *ATP8B1* and *C1orf116*, the human orthologue of candidate gene *AA986860*, was reported in rod photoreceptors or RPE cells of human retina, and no transcripts of *Atp8b1* was identified in mouse rods and/or RPE cells (Supplementary Fig.2). The lack of gene expression reported by the Plae database may be because of the low expression of the gene of interest, which could not be detected by scRNA-seq analysis, or there is no expression at all. Additionally, the investigation through the gEAR²⁶ database revealed the expression of all candidate genes and human USH genes in the inner ear HCs of both mice and humans (18/18 candidate genes, 15/15 USH genes) (Supplementary Fig.3-8).

PROTEIN INTERACTION ANALYSIS

We sought to predict if any protein encoded by the 18 human orthologues of candidate genes interact with any encoded protein among the 15 human USH genes, the 39 genes associated with other inherited DSI syndromes derived from Guimaraes and colleagues, 2023,² or the 263 known ciliopathy genes, a combination of Syscilia and Ciliacarta, from Higgins and coworkers, 2022.³¹ *MT-TL1* from other inherited DSI (a causative mitochondrial gene of maternally-inherited diabetes and deafness, coding for a leucine tRNA⁴⁷) and *PTCHD3* from ciliopathy genes are not represented in the STRING-db^{19,20} and thus could not be analyzed.

No known protein-protein interaction between the 18 candidates and 15 human USH genes, or between the 18 candidates and other 38 inherited DSI genes, was found (Figure 1B). Notably, we found that FER and DYRK1B, both from our 18 candidate list, interact with CTNNB and DCAF from the ciliopathy list, respectively. To further explore the protein-protein interactions present between the candidates and other gene collections, the confidence level was reduced to 0.7. With this confidence level, three new interactions were noted between protein products of *CSTB*, *SPRED1* and *XRCC5* of candidate genes with *TRAPPC10*, *RAF1* and *ORC1* of ciliopathy genes, respectively. (Supplementary Fig.9).

MOLECULAR FUNCTIONS AND SIGNALING PATHWAYS ANALYSIS

We used bioinformatic tools to identify relationships between the molecular functions and signaling pathways in our candidate gene set and sets of human USH, and other established DSI genes. The PANTHER classification system^{21,22} shows the existence of three similar molecular functions shared among our candidate

genes, the human USH genes, and other inherited DSI genes: ATP-dependent activity, binding and catalytic activity. Molecular function regulator and molecular transducer activities are only shared between the gene profile of candidates and other inherited DSI. Additionally, each gene set was found to have unique molecular functions. Candidate genes (Fig.2A) were uniquely associated with molecular adaptor and transporter activities while only human USH genes were associated with cytoskeletal motor activity (Fig.2B). Additionally, other (non-USH) inherited DSI syndrome genes uniquely participated in structural molecule and transcription regulator activities (Fig.2C).

We employed DAVID^{23,24} to study the related pathways in which the candidate genes and the two other gene sets contribute. Three different signaling pathway databases were studied in this bioinformatic tool: KEGG, Reactome, and WIKI pathways. KEGG revealed that candidate genes shared the lysosome pathway with human USH genes, while the adherens junction and cytoskeleton in muscle cells pathway were shared by the candidate gene set and inherited DSI genes. WIKI pathways showed no additional signaling pathway similarities (Supplementary data sheet 1).

According to Reactome, four pathways were common between the three gene sets: metabolism of proteins, signal transduction, post-translational protein modification, and cell cycle. Moreover, metabolism pathway was linked to both the candidate genes and human USH genes, while the candidate and inherited DSI genes shared immune system, innate immune system, neutrophil degranulation, signaling by receptor tyrosine kinases and cytosolic sensors of pathogen-associated DNA pathways (Table 4). *MT-TL1*, an inherited DSI gene, was not represented in the DAVID and PANTHER database and thus could not be analyzed.

CORRESPONDENCE OF CANDIDATE GENES WITH UNSOLVED HUMAN USH LOCI

So far, three human USH loci of unidentified genes, evident by mapping linkage, have been associated with USH1.^{2,6} These loci are 10p11.21-q21.1, 15q22-q23, and 21q21. An analysis using the GeneCards database^{17,18} revealed three human orthologs of our candidate genes are adjacent to these loci: *SPRED1* at 15q14, *CHSY1* at 15q26.3, and *CSTB* at 21q22.3. Future work is needed to determine if these candidates are related to USH1.

ASSOCIATION OF CANDIDATE GENES WITH RETINOPATHY OR DEAFNESS

To further validate our candidate genes, we screened RetNet,²⁸ SHIELD,²⁹ and DVD³⁰ to identify any association between our candidate genes with inherited retinal diseases (IRDs) and/or deafness in human populations.

Among human orthologs of our candidate gene set, *ATP8B1* is within CORD1 locus, *MPDZ* can cause AR macular degeneration, and *ADIPOR1* is known to cause recessive syndromic retinopathy as part of BBS, autosomal dominant (AD) RP, and syndromic/systemic diseases with retinopathy (AR).

In terms of hearing disability, pathogenic variants in *IDUA* were associated with hearing impairment in a patient with Hurler-Scheie syndrome.⁴⁸ *RNF10* is within mapped loci of DFNA25 and DFNA41. In addition, *CHSY1* is associated with both the DFNA30 and OTSC1 loci. Furthermore, missense variants of *CHSY1* may be causative of hearing impairment.⁴⁹

Mpdz KO MOUSE MODEL, ONE OF THE CANDIDATE GENES FOR INHERITED DSI SYNDROME

Based on the IMPC database, the *Mpdz*^{-/-} mouse showed abnormal retina morphology, defined by structural anomaly of the neural retina, along with abnormal retinal blood vessels and vasculature morphology, compared to the WT mice (Fig.3A & 3B). Additionally, ERG recordings revealed significant reduction in cone b-wave, rod b-wave, and rod a-wave amplitudes ($p < .0001$, Fig.3C). ABR test results (Fig.3D), conducted by the IMPC revealed that mutant mice were associated with reduced hearing, evident by increased ABR threshold. The increase in ABR threshold is evident across all frequencies tested (6 kHz-30 kHz). The KO was tested in the early adult stage of life. Retinal transcriptomic data from the Plae²⁵ database illustrated the expression of this gene in both human and mouse retina (Supplementary Fig.2), specifically in rod photoreceptors and/or RPE cells. The expression of *Mpdz* in the mouse and human inner ear HCs (Supplementary Fig.4,7,8) are demonstrated by the gEAR database.²⁶

According to the IMPC database, mice lacking *Mpdz* exhibit abnormalities in other physiological systems: homeostasis/metabolism (improved glucose tolerance, increased circulating potassium level), behavior/neurological (decreased grip strength, decreased startle reflex), growth/size/body region and cardiovascular system (increased

heart weight). As the Charge syndrome symptoms include hearing loss, retinal and macula coloboma, retarded growth/development and heart disease², the *Mpdz* KO mouse could be a model for this syndrome. Similarly, this gene can be considered as a possible candidate for Kearns-Sayre syndrome, and maternally-inherited diabetes and deafness, due to the cardiac and behavior/neurological abnormalities seen in *Mpdz*^{-/-} mouse line. Although the abnormal phenotypes from loss of this gene do not exactly phenocopy the Charge, Kearns-Sayre syndrome, and maternally-inherited diabetes and deafness syndromes, they share significant similarities, which suggests a potential link with them.

IMPC HISTOPATHOLOGY

The IMPC histopathological analysis of the retina on a subset of the lines from the candidate genes, showed definite abnormalities consistent with the clinical phenotyping findings. A comparison of the retina in the WT and *Idua*^{-/-} mice showed reduced thickness in outer nuclear layer and retina of *Idua*^{-/-} mice (Fig.4A-C). Similarly, compared to WT, severe outer retinal atrophy, including the outer nuclear layer where rod nuclei are located, was detected in *Chsy1*^{-/-} mice (Fig.4D & 4E). However, not all IMPC *in vivo* testing is corroborated by histopathology. For example, the comparison between WT and *Chsy1*^{-/-} organ of Corti showed no obvious abnormality by routine histopathology (Fig.4F & 4G) despite abnormal ABR test results (Supplementary Fig1). Retinal lamination defects were observed in the outer retina of *Fer*^{-/-} and *Fer*^{+/-} mice, but they were interpreted to be more likely due to the *rd8* mutation present in C57BL/6N mice, the background used by the IMPC⁵⁰ (Supplementary Fig.10A-10C). However, color fundus imaging of *Fer* mutant mice showed abnormal lesions which were different than the *rd8* phenotype (Supplementary Fig.11A-11C). Similarly, the retina and inner ear of *Eef1d*^{+/-} mice showed no obvious histopathologic abnormality (Supplementary Fig.10D-10F) despite showing signs of abnormal retinal morphology on slit lamp and ophthalmoscope examinations with abnormal ABR test result, reported by IMPC. Although there is no available retinal or inner ear histopathology imaging of *Xrcc5*, *Spred1*, and *Rnf10* KO mice, fundus images showed abnormal retinal blood vessel pattern in all three lines with retinal degeneration only seen in *Xrcc5* and *Spred1* KO mice (Supplementary Fig.11D-11H). Comparison of ERG studies on WT and *Rnf10*^{-/-} mice revealed that amplitude of rod a-wave and rod b-wave are significantly reduced in *Rnf10*^{-/-} mice (Supplementary Fig.11I, *p*=.0278 & 11J, *p*<.0001).

Sclt1 KO MOUSE, AS A MODEL OF BBS

BBS is a DSI syndrome and ciliopathy, similar to USH, which manifests as retinal degeneration, hearing difficulty, renal dysfunction, obesity, hypogonadism, postaxial polydactyly and cognitive impairment, typically with an autosomal recessive inheritance.² During our screening of IMPC KO mouse lines,⁹⁻¹⁵ we noticed that knocking out *Sclt1*, a putative ciliopathy gene,³¹ led to posterior synechiae, retinal degeneration, polycystic kidney, and polydactyly (Fig.5) confirmed by histopathology. Additionally, the gEAR database reported the expression of this gene in the inner ear HCs of both human and mouse.²⁶

According to DAVID/Reactome, signaling pathways in which *SCLT1* contributes are cilium assembly, anchoring of the basal body to the plasma membrane, and organelle biogenesis and maintenance. These pathways are similar to the signaling pathways of confirmed BBS causative genes.^{2,23,24}

Sclt1 homozygous KOs (HOM) are sub-viable, with fewer than 12.5% of HOM surviving to genotyping age and all HOM mice died or were euthanized around 3 weeks of age. Only histology/histopathology studies were done on KO mice. The results of HET mice examinations for retinal and hearing phenotypes were not significant, consistent with an autosomal recessive mode of inheritance observed in BBS. Also, in a previously published study done by Morisada and associates, 2022,⁵¹ identical compound heterozygous SCLT1 mutation was reported in two unrelated patients with clinical diagnosis of BBS.⁵¹ Therefore, *Sclt1* mutant mice might be a good model for BBS due to phenotyping similarities with this syndrome. It would be informative to test a patient-specific variant on this background using a conditional model and/or this allele in a different strain background to see if the mice live long enough to undergo in-life phenotyping.

SLC20A2 IS A CANDIDATE GENE FOR USHER SYNDROME

Genome sequencing (GS) in 230 unsolved IRD cases identified one Usher syndrome proband (OGI767_1502) with a heterozygous rare variant (c.215A>C; p.Lys72Thr) in exon 2 of the Solute Carrier Family 20 Member 2 (*SLC20A2*) gene, a human orthologue of one of the 18 mouse candidate genes, encoding a member of the

inorganic phosphate transporter family (Fig.6A). Variants in this gene have been previously associated with dominant primary familial brain calcification (also known as Fahr's syndrome, OMIM 213600) that manifests with parkinsonism.⁵² Sanger sequencing confirmed the presence of the p.Lys72Thr variant in the proband and excluded it from his unaffected mother and maternal half-sister (Fig.6A). However, as the DNA from the reported unaffected father was not available, we could neither confirm a *de novo* inheritance nor an autosomal dominant inheritance with incomplete penetrance. A known pathogenic heterozygous variant (c.5237G>A; p.Arg1746Gln) in *CDH23*, a gene associated with recessive Usher syndrome type 1, was also identified on panel-based testing and confirmed on GS, but no second allele was found. Likewise, pathogenic variants in other USH-associated genes were excluded.

The *SLC20A2* c.215A>C; p.Lys72Thr missense variant was absent from GnomAD v4 population database (<https://gnomad.broadinstitute.org>),⁵³ as well as LOVD⁵⁴ and ClinVar⁵⁵ databases, both containing curated patient variant data. The p.Lys72Thr was predicted to be likely causal by several in-silico predictors (CADD score: 24.9; REVEL: 0.809; AlphaMissense: 0.644, MetaDome Mutation Intolerance: 0.21) but not by SpliceAI (score = 0), suggesting that the underlying pathogenic mechanism is unlikely to affect splicing. Additionally, modelling of the p.Lys72Thr change using ChimeraX on the AlphaFold predicted structure of SLC20A2 protein, we observed that the introduced threonine at residue 72, is predicted to disrupt a hydrogen bond with the glutamine residue at position 528 and generate an additional hydrogen bond with the glutamic acid residue at position 68, thus suggesting a change in protein folding (Fig.6B).

OGI767_1502 is a 66-year-old male diagnosed with Usher syndrome type 1 secondary to profound congenital sensorineural hearing impairment and RP. He was initially diagnosed with RP at age 19 with complaints of decreased night and peripheral vision loss at that time. At age 20, corrected visual acuity was 20/30 in the right eye (OD) and 20/30 in the left eye (OS) with fundus findings typical of RP. Full-field electroretinography at age 20 showed near-nondetectable responses to scotopic bright flash and nondetectable responses to the 30 Hz stimulus. Goldmann perimetry at age 21 was reported to show constriction in each eye to 10-15° and 15-20° to the I4e and V4e targets respectively. ERG was later repeated with bandpass filtering and signal averaging to enable detection of 30 Hz responses: at age 35, responses were 1.4 uV OD and 1.6 uV OS with prolonged implicit times while at age 56, responses had decreased to 0.68 uV OD and 0.91 uV OS. At age 66, visual acuity had decreased to 20/100 OD and 20/200 OS with dry eye and cataract also being contributory factors. Fundus exam continued to show typical features of RP (Fig.6C), while fundus autofluorescence (FAF) of the right eye showed preserved FAF in the central macula but diffuse reduction and absence of FAF in the peripheral macula extending through the visible periphery (Fig.6D). Goldmann perimetry using the I4e and V4e targets revealed generalized constriction of 10° and 20° degrees, respectively. Optical coherence tomography of the right eye showed outer retinal bands, including ellipsoid zone, present centrally but attenuated in the peripheral macula. Cystoid macular edema was also present and that was treated with acetazolamide. His medical history also included learning disability and Parkinson's disease with the latter diagnosed after age 60. As variants in *SLC20A2* are known to cause the parkinsonism seen in Fahr's syndrome, the novel c.215A>C; p.Lys72Thr may underlie the patient's neurologic condition and may also lead to the USH1 symptoms, though with the current genetic evidence it is classified as variant of uncertain significance (VUS).

DISCUSSION

By analyzing different mutant mouse lines, we aimed to identify novel DSI - associated candidate genes, their molecular functions, and signaling pathways. Our goal was to provide justification for research to determine disease causality, expand the genetic diagnosis in currently unsolved patients, and identify novel genotype-phenotype associations.

We found 18 novel candidate genes associated with hearing and retinal phenotypes in mouse KO lines. All of these lines also demonstrated effects on other physiological systems, expanding the scope of our study to other causes of inherited DSI beyond USH. The abnormal constellation of phenotypes manifested in different physiological systems do not fully overlap with human disease owing to species-specific differences and the "snapshot-in-time" approach of the IMPC phenotyping pipeline. It is also possible that human patients may not undergo as comprehensive systemic phenotyping as mouse models. Human mutations may also be hypomorphic or neomorphic rather than loss-of-function alleles in mouse knockouts, since the latter are targeted deletions predicted to lack all gene function. Also, inherited DSI syndromes are relatively uncommon in humans and may not yet be fully characterized. For instance, there have been reports of bronchiectasis, somatosensory deficit, reduced sperm motility, and olfactory loss in USH patients.⁵ Therefore, our candidate gene set could be considered for both USH and other inherited DSI syndromes. Finally, OMIM database has reported on 11 out of 18 candidate genes that were

identified to have known association with other non-sensory phenotypes, mostly neurodevelopmental disorders (Supplementary table 1), six of which are reported to impair vision and/or hearing in a subset of patients. Ophthalmic involvement in *PIGQ* patients includes vertical nystagmus, hyperopia, astigmatism, cortical visual impairment; *IDUA* mutation led to retinal degeneration which commonly occurs in Mucopolysaccharidosis type I and hearing impairment in a Hurler-Scheie syndrome patient; *ANKRD11* and *CHSY1* were associated with mixed hearing loss and sensorineural hearing loss, respectively; patients with *MPDZ* mutation had retinal involvement including foveal dysplasia with thin inner retina, and sensorineural hearing loss; *EEF1D* patients were reported to have optic atrophy in three patients, and retinal pigmentary abnormalities in one. Phenotypic differences could be due to allele type and/or genetic background differences that modify gene function.

One of the human orthologues leading to non-sensory phenotypes is *SLC20A2*, causing dominant primary familial brain calcification (also known as Fahr's syndrome), a condition that manifests with parkinsonism. The OMIM database has also reported on early-onset epilepsy, developmental delay, and mental retardation in patients harboring *SLC20A2* mutations. In one patient with USH1 and parkinsonism manifested at typical onset (over 60 years old), we identified a rare missense variant in this gene, p.Lys72Thr, predicted as likely causal. This variant has never been reported in any patient with Fahr's syndrome and on ClinVar, the only missense variant affecting the same position (p.Lys72Arg) has been classified as VUS, after being reported as part of a commercial genetic panel for inborn genetic diseases. Despite the interesting genetic finding in our patient, the lack of further USH1 patients with variants in *SLC20A2* and its clear association with Fahr's syndrome do not allow us to fully present this finding as a novel genetic association, but rather as a candidate gene for USH1. Therefore, recognizing known disease associations for these candidate genes using existing genetic databases remains a crucial step to validate any novel association and propose a candidate gene for genetic testing panels.

The literature search on KO and/or HET mouse lines of USH genes and inherited DSI genes revealed that mouse lines of other non-USH inherited DSI genes showed higher fidelity regarding retinopathy, suggesting that these genes could affect parts of the photoreceptors which may be similar between humans and mice. This observation supports the conclusion that USH genes likely participate in calyceal processes and the periciliary membrane which are more prominent in primate photoreceptors than in those of rodents. However, other DSI genes may function in other photoreceptor compartments which may be more similar amongst these species. Since our candidate genes frequently had additional phenotypes beyond retinal and hearing abnormalities, we expect a minority of genes responsible for USH, with most being associated with other DSI syndromes.

Investigating the cellular expression of USH genes and our candidate gene set in both species revealed no expression of some of the established USH genes (*USH1G*, *CLRN1*) in either rods or RPE cells of human retina. Nevertheless, the mutation of either of these genes causes RP as part of the USH phenotype. Therefore, we conclude that some bona fide disease-causing genes may escape the resolution of single-cell transcriptomics. Accordingly, the expression of the *C1orf116* and *ATP8B1* was neither detected in RPE cells nor rod photoreceptors. This could be due to low level of expression, or due to cell-non-autonomous effects; however, the absence of expression of these genes does not preclude a role for them in disease.

Protein interaction analysis of our gene sets revealed two interactions between proteins encoded by candidates (*DYRK1B* and *FER*) and ciliopathy genes. Dual-specificity tyrosine-regulated kinase (*DYRK*) family and *FER* are both evolutionarily conserved genes.^{56,57} Cell proliferation, apoptosis, differentiation and survival are managed by the DYRK family through altering the protein activation status, cellular localization and turn-over.⁵⁶ Other DYRKs have been involved in regulating the primary cilium (10.1038/s42003-025-08373-5); *DYRK1B* modulates the activity and protein stability of GLI transcription factors, which are critical mediators of the Hedgehog signal that operates through primary cilia (10.18632/oncotarget.13662; 10.2337/db25-196-OR). *FER* is a non-transmembrane receptor tyrosine kinase within the *fes/fps* family with ubiquitous expression.⁵⁷ This gene participates in cell survival, cytoskeleton rearrangement, epithelial maintenance, and leukocyte differentiation and chemotaxis.⁵⁷ *FER* is involved in ciliary function and hence may cause DSI. The other 16 candidates we identified do not have predicted interactions with ciliopathy or DSI proteins or with one another at 0.9 confidence level, despite being expressed in rods and hair cells. This finding suggests that this cohort of relatively understudied genes may underlie heretofore unappreciated mechanisms of DSI such as USH. Accordingly, bioinformatic study pointed to novel functions of candidate genes that were not present amongst USH and other DSI gene sets. The gene ontology analysis indicated that the candidate gene set is involved in "molecular adaptor activity" (GO:0060090) and "transporter activity" (GO:0005215). These GO terms were not found among existing USH or other DSI gene sets. Subsequent study of candidate genes will elucidate their role in sensory neurons and also the degree to which they affect vision and hearing in people.

Through our literature review, we observed that some of the USH patients with mutations in the scaffold *USH1C*, which is a confirmed USH1 gene, exhibit severe inflammatory enteropathy and nephropathy along with vision and auditory loss. *USH1C* is shared between the intermicrovillar adhesion complex (IMAC), a complex required for proper organization of enterocytes' apical microvilli in the form of brush border, and USH complex although the splice isoforms used between the two complexes varies.⁵⁸ *CALML4*, a novel IMAC component, is highly expressed at the distal tips of enterocytes' microvilli and stereocilia of HCs, the main action site of IMAC and USH complex, respectively. Co-immunoprecipitation experiments in a published study showed that this gene functions as a light chain by interacting with the neck region of both *MYO7B* in IMAC and *MYO7A* in USH complex.⁵⁸ Additionally, in a genome-wide linkage screen performed on two consanguineous Pakistani families with USH1 phenotype, *CALML4* is reported within the USH1H locus.⁵⁹ Thus, a mutation in this gene may result in USH1H. Future studies on *Calml4* KO mice generated by the IMPC will help clarify this issue.

Studying retinal abnormalities using IMPC mice is complicated by the presence of the *Crb1^{rd8}* variant in C57BL/6N mice, the background on which all IMPC mice were generated,⁶⁰ that is associated with a slowly progressive photoreceptor degeneration.⁶¹ To mitigate the number of false positive hits during eye screening, phenotyping staff were trained to distinguish the background level of retinal dysplasia in *Crb1^{rd8}* mice. The examiners were also masked to the genotype of the mice, and WT mice are mixed in with KO animals. We consider the retinal hits identified by IMPC phenotyping to be a sensitized screen with an overrepresented proportion of lines with abnormal retinas, some of which may be genetic modifiers of *Crb1*.⁶² Some of these KO lines may not have any retinal abnormality independent of *Crb1^{rd8}*,⁵⁰ which is a limitation of this study. To maximize the rigor of this study and minimize the chance of false positive genes, we imposed an additional threshold of only including mouse lines which had bilaterally symmetric retinal findings. Nevertheless, some lines such as *Fer* and *Eef1d* could not be corroborated with routine histopathological studies. As all test elements of the IMPC phenotyping process are performed at a single time point, more comprehensive longitudinal evaluation of the *Eef1d* and *Fer* lines may show more alterations in retinal and/or inner ear histopathology. Similarly, the onset of symptoms in different types of USH varies from the appearance of RP within the first decade of life and typically congenital SNHL in USH1 patients, to the appearance of USH4 symptoms, usually around 40 years of age.² *EEF1D*⁶³ and *PIGQ*⁶⁴ mutations have been previously associated with retinopathies in patients. Furthermore, ATP8B1 deficiency in patients was reported to cause hearing loss.⁴³ All were not mentioned on RetNet, DVD or SHIELD database, highlighting the importance of further studies on our candidate genes list.

Our study highlights the power of mouse models to find novel causative genes for human diseases, including inherited retinopathies and deafness. This strategy contributes to a greater understanding of the related molecular functions and signaling pathways underlying single gene disorders and promotes enhanced genetic diagnosis. Furthermore, we recognized known disease associations of the candidate genes. We advocate using existing genetic databases to further assess any human correlations before adding the candidate genes to genetic testing panels. We would also strongly suggest that this study is an example of discoveries that can only be made using an in vivo model, and that cannot be replaced by a novel alternative methodology or other non-in vivo systems.

ABBREVIATIONS

USH	Usher Syndrome
RP	Retinitis Pigmentosa
SNHL	Sensorineural Hearing Loss
HC	Hair Cell
RPE	Retinal Pigment Epithelium
WT	Wild-type
KO	Knockout
IMPC	International Mouse Phenotyping Consortium
ABR	Auditory Brainstem Response
ERG	Electroretinogram
PlaE	PLatform for Analysis of scEiad
gEAR	gene Expression Analysis Resource
DAVID	Database for Annotation, Visualization and Integrated Discovery
DVD	Deafness Variation Database
SHIELD	Shared Harvard Inner Ear Laboratory Database

RetNet	Retinal information Network
SnRNA-seq	Single nucleus RNA-sequencing
ScRNA-seq	Single cell RNA-sequencing
VUS	Variant of Uncertain Significance

ACKNOWLEDGMENTS

We want to thank all members of the Medical Research Council (MRC) Harwell Institute, Helmholtz Munich (HMGU), Model Animal Research Center (MARC), Institute of Molecular Genetics (IMG), Wellcome Trust Sanger Institute (WTSI), Institut Clinique de la Souris (ICS)— PHENOMIN-ICS, Baylor College of Medicine (BCM), The Jackson Laboratory (JAX), The Center for Phenogenomics (TCP) and University of California, Davis (UC Davis). Work of the HMGU was supported by Infrafrontier grant 01KX1012; EU Horizon2020: IPAD-MD funding 653961 (MHdA). The authors used services of the Czech Centre for Phenogenomics at the IMG, supported by the Czech Academy of Sciences RVO 68378050 and by the projects LM2023036, CZ.02.1.01/0.0/0.0/16_013/0001789 as well as CZ.02.1.01/0.0/0.0/18_046/0015861, provided by the Ministry of Education, Youth and Sports of the Czech Republic. The work of PHENOMIN-ICS was supported in part by IdEx Unistra (ANR-10-IDEX-0002), SFRI-STRAT'US project (ANR-20-SFRI-0012), INBS PHENOMIN (ANR-10-IDEX-0002-02) under the framework of the France 2030 Program to YH. Additionally, this work was supported by grants from the National Eye Institute [R01EY035717 (KMB), and P30EY014104 (MEEI core support)], Iraty Award 2023 (KMB), Lions Foundation (KMB), Research to Prevent Blindness Unrestricted Grant (KMB), the Curing Kids Foundation (KMB), and Foundation Fighting Blindness Career Development Award (RMH).

The authors would like to thank the patient and their family members for their participation in this study and the Ocular Genomics Institute Genomics Core members for their experimental assistance.

REFERENCES

- Swenor BK, Ramulu PY, Willis JR, Friedman D, Lin FR. The prevalence of concurrent hearing and vision impairment in the United States. *JAMA internal medicine*. 2013;173(4):10.1001/jamainternmed.2013.1880. doi:10.1001/jamainternmed.2013.1880
- Guimaraes TAC de, Arram E, Shakarchi AF, Georgiou M, Michaelides M. Inherited causes of combined vision and hearing loss: clinical features and molecular genetics. *British Journal of Ophthalmology*. 2023;107(10):1403-1414. doi:10.1136/bjo-2022-321790
- Mathur P, Yang J. Usher syndrome: Hearing loss, retinal degeneration and associated abnormalities. *Biochimica et Biophysica Acta (BBA) - Molecular Basis of Disease*. 2015;1852(3):406-420. doi:10.1016/j.bbadis.2014.11.020
- Delmaghani S, El-Amraoui A. The genetic and phenotypic landscapes of Usher syndrome: from disease mechanisms to a new classification. *Human Genetics*. 2022;141(3-4):709. doi:10.1007/s00439-022-02448-7
- Fuster-García C, García-Bohórquez B, Rodríguez-Muñoz A, et al. Usher Syndrome: Genetics of a Human Ciliopathy. *Int J Mol Sci*. 2021;22(13):6723. doi:10.3390/ijms22136723
- Castiglione A, Möller C. Usher Syndrome. *Audiol Res*. 2022;12(1):42-65. doi:10.3390/audiolres12010005
- Sahly I, Dufour E, Schietroma C, et al. Localization of Usher 1 proteins to the photoreceptor calyceal processes, which are absent from mice. *J Cell Biol*. 2012;199(2):381-399. doi:10.1083/jcb.201202012
- Williams DS. Usher syndrome: animal models, retinal function of Usher proteins, and prospects for gene therapy. *Vision research*. 2007;48(3):433. doi:10.1016/j.visres.2007.08.015
- Groza T, Gomez FL, Mashhadi HH, et al. The International Mouse Phenotyping Consortium: comprehensive knockout phenotyping underpinning the study of human disease. *Nucleic Acids Research*. 2023;51(D1):D1038-D1045. doi:10.1093/nar/gkac972
- Dickinson ME, Flenniken AM, Ji X, et al. High-throughput discovery of novel developmental phenotypes. *Nature*. 2016;537(7621):508-514. doi:10.1038/nature19356
- Birling MC, Yoshiki A, Adams DJ, et al. A resource of targeted mutant mouse lines for 5,061 genes. *Nat Genet*. 2021;53(4):416-419. doi:10.1038/s41588-021-00825-y
- Elrick H, Peterson KA, Willis BJ, et al. Impact of essential genes on the success of genome editing experiments generating 3313 new genetically engineered mouse lines. *Sci Rep*. 2024;14(1):22626. Published 2024 Sep 30. doi:10.1038/s41598-024-72418-8
- Bowl MR, Simon MM, Ingham NJ, et al. A large scale hearing loss screen reveals an extensive unexplored

- genetic landscape for auditory dysfunction. *Nat Commun.* 2017;8:886. doi:10.1038/s41467-017-00595-4
14. Moore BA, Leonard BC, Sebbag L, et al. Identification of genes required for eye development by high-throughput screening of mouse knockouts. *Commun Biol.* 2018;1:236. doi:10.1038/s42003-018-0226-0
 15. Haselimashhadi H, Mason JC, Mallon AM, Smedley D, Meehan TF, Parkinson H. OpenStats: A robust and scalable software package for reproducible analysis of high-throughput phenotypic data. *PLOS ONE.* 2020;15(12):e0242933. doi:10.1371/journal.pone.0242933
 16. Percie du Sert N, Hurst V, Ahluwalia A, et al. The ARRIVE guidelines 2.0: Updated guidelines for reporting animal research. *PLoS Biol.* 2020;18(7):e3000410. Published 2020 Jul 14. doi:10.1371/journal.pbio.3000410
 17. Stelzer G, Rosen N, Plaschkes I, et al. The GeneCards Suite: From Gene Data Mining to Disease Genome Sequence Analyses. *Current Protocols in Bioinformatics.* 2016;54(1):1.30.1-1.30.33. doi:10.1002/cpbi.5
 18. Safran M, Rosen N, Twik M, et al. The GeneCards Suite. In: Abugessaisa I, Kasukawa T, eds. *Practical Guide to Life Science Databases.* Springer Nature; 2021:27-56. doi:10.1007/978-981-16-5812-9_2
 19. Szklarczyk D, Kirsch R, Koutrouli M, et al. The STRING database in 2023: protein–protein association networks and functional enrichment analyses for any sequenced genome of interest. *Nucleic Acids Res.* 2022;51(D1):D638-D646. doi:10.1093/nar/gkac1000
 20. Doncheva NT, Morris JH, Gorodkin J, Jensen LJ. Cytoscape StringApp: Network Analysis and Visualization of Proteomics Data. *J Proteome Res.* 2019;18(2):623-632. doi:10.1021/acs.jproteome.8b00702
 21. Thomas PD, Ebert D, Muruganujan A, Mushayahama T, Albou LP, Mi H. PANTHER: Making genome-scale phylogenetics accessible to all. *Protein Science.* 2022;31(1):8-22. doi:10.1002/pro.4218
 22. Mi H, Muruganujan A, Huang X, et al. Protocol Update for large-scale genome and gene function analysis with the PANTHER classification system (v.14.0). *Nat Protoc.* 2019;14(3):703-721. doi:10.1038/s41596-019-0128-8
 23. Huang DW, Sherman BT, Lempicki RA. Systematic and integrative analysis of large gene lists using DAVID bioinformatics resources. *Nat Protoc.* 2009;4(1):44-57. doi:10.1038/nprot.2008.211
 24. Huang DW, Sherman BT, Lempicki RA. Bioinformatics enrichment tools: paths toward the comprehensive functional analysis of large gene lists. *Nucleic Acids Res.* 2009;37(1):1-13. doi:10.1093/nar/gkn923
 25. Swamy VS, Fufa TD, Hufnagel RB, McGaughey DM. Building the mega single-cell transcriptome ocular meta-atlas. *GigaScience.* 2021;10(10):giab061. doi:10.1093/gigascience/giab061
 26. Orvis J, Gottfried B, Kancherla J, et al. gEAR: Gene Expression Analysis Resource portal for community-driven, multi-omic data exploration. *Nat Methods.* 2021;18(8):843-844. doi:10.1038/s41592-021-01200-9
 27. van der Valk WH, van Beelen ESA, Steinhart MR, et al. A single-cell level comparison of human inner ear organoids with the human cochlea and vestibular organs. *Cell Rep.* 2023;42(6):112623. doi:10.1016/j.celrep.2023.112623
 28. Daiger SP, Rossiter BJ, Greenberg J, Christoffels A, Hide W. Data services and software for identifying genes and mutations causing retinal degeneration. *Investigative Ophthalmology and Visual Science.* 1998; 39(Suppl): S295
 29. Shen J, Scheffer DI, Kwan KY, Corey DP. SHIELD: an integrative gene expression database for inner ear research. *Database: The Journal of Biological Databases and Curation.* 2015;2015:bav071. doi:10.1093/database/bav071
 30. Azaiez H, Booth KT, Ephraim SS, et al. Genomic Landscape and Mutational Signatures of Deafness-Associated Genes. *The American Journal of Human Genetics.* 2018;103(4):484-497. doi:10.1016/j.ajhg.2018.08.006
 31. Higgins K, Moore BA, Berberovic Z, et al. Analysis of genome-wide knockout mouse database identifies candidate ciliopathy genes. *Sci Rep.* 2022;12:20791. doi:10.1038/s41598-022-19710-7
 32. Scott HA, Place EM, Ferenchak K, et al. Expanding the phenotypic spectrum in RDH12-associated retinal disease. *Cold Spring Harb Mol Case Stud.* 2020;6(1):a004754. Published 2020 Feb 3. doi:10.1101/mcs.a004754
 33. Moye AR, Bedoni N, Cunningham JG, et al. Mutations in ARL2BP, a protein required for ciliary microtubule structure, cause syndromic male infertility in humans and mice. *PLoS Genet.* 2019;15(8):e1008315. Published 2019 Aug 19. doi:10.1371/journal.pgen.1008315
 34. Haer-Wigman L, Newman H, Leib R, et al. Non-syndromic retinitis pigmentosa due to mutations in the mucopolysaccharidosis type IIC gene, heparan-alpha-glucosaminide N-acetyltransferase (HGSNAT). *Hum Mol Genet.* 2015;24(13):3742-3751. doi:10.1093/hmg/ddv118
 35. Men CJ, Bujakowska KM, Comander J, et al. The importance of genetic testing as demonstrated by two cases of CACNA1F-associated retinal generation misdiagnosed as LCA. *Mol Vis.* 2017;23:695-706. Published 2017

Oct 10.

36. Collins RL, Brand H, Karczewski KJ, et al. A structural variation reference for medical and population genetics [published correction appears in *Nature*. 2021 Feb;590(7846):E55. doi: 10.1038/s41586-020-03176-6.].
37. Lewandowski D, Foik AT, Smidak R, et al. Inhibition of ceramide accumulation in AdipoR1^{-/-} mice increases photoreceptor survival and improves vision. *JCI Insight*. 2022;7(4):e156301. Published 2022 Feb 22. doi:10.1172/jci.insight.156301
38. Macke EL, Henningsen E, Jessen E, et al. Loss of Chondroitin Sulfate Modification Causes Inflammation and Neurodegeneration in skt Mice. *Genetics*. 2020;214(1):121-134. doi:10.1534/genetics.119.302834
39. Liu Y, Xu L, Hennig AK, et al. Liver-directed neonatal gene therapy prevents cardiac, bone, ear, and eye disease in mucopolysaccharidosis I mice. *Mol Ther*. 2005;11(1):35-47. doi:10.1016/j.ymthe.2004.08.027
40. Albrecht NE, Alevy J, Jiang D, et al. Rapid and Integrative Discovery of Retina Regulatory Molecules. *Cell Rep*. 2018;24(9):2506-2519. doi:10.1016/j.celrep.2018.07.090
41. Yu J, Lei K, Zhou M, et al. KASH protein Syne-2/Nesprin-2 and SUN proteins SUN1/2 mediate nuclear migration during mammalian retinal development. *Hum Mol Genet*. 2011;20(6):1061-1073. doi:10.1093/hmg/ddq549
42. Karanjawala ZE, Hinton DR, Oh E, Hsieh CL, Lieber MR. Developmental retinal apoptosis in Ku86^{-/-} mice. *DNA Repair (Amst)*. 2003;2(12):1429-1434. doi:10.1016/j.dnarep.2003.08.011
43. Stapelbroek JM, Peters TA, van Beurden DH, et al. ATP8B1 is essential for maintaining normal hearing. *Proc Natl Acad Sci U S A*. 2009;106(24):9709-9714. doi:10.1073/pnas.0807919106
44. Schachern PA, Cureoglu S, Tsuprun V, Paparella MM, Whitley CB. Age-related functional and histopathological changes of the ear in the MPS I mouse. *Int J Pediatr Otorhinolaryngol*. 2007;71(2):197-203. doi:10.1016/j.ijporl.2006.09.016
45. Jarysta A, Tarchini B. Multiple PDZ domain protein maintains patterning of the apical cytoskeleton in sensory hair cells. *Development*. 2021;148(14):dev199549. doi:10.1242/dev.199549
46. Horn HF, Brownstein Z, Lenz DR, et al. The LINC complex is essential for hearing. *J Clin Invest*. 2013;123(2):740-750. doi:10.1172/JCI66911
47. Campbell T, Lou X, Slone J, et al. Mitochondrial genome variant m.3250T>C as a possible risk factor for mitochondrial cardiomyopathy. *Hum Mutat*. 2021;42(2):177-188. doi:10.1002/humu.24143
48. Teng YN, Wang TR, Hwu WL, Lin SP, Lee-Chen GJ. Identification and characterization of -3c-g acceptor splice site mutation in human alpha-L-iduronidase associated with mucopolysaccharidosis type IH/S. *Clin Genet*. 2000;57(2):131-136. doi:10.1034/j.1399-0004.2000.570207.x
49. Schrauwen I, Melegh BI, Chakchouk I, et al. Hearing impairment locus heterogeneity and identification of PLS1 as a new autosomal dominant gene in Hungarian Roma. *Eur J Hum Genet*. 2019;27(6):869-878. doi:10.1038/s41431-019-0372-y
50. Kwon YS, Tham A, Lopez AJ, et al. Cytoglobin deficiency potentiates Crb1-mediated retinal degeneration in rd8 mice. *Developmental biology*. 2019;458(2):141. doi:10.1016/j.ydbio.2019.10.013
51. Morisada N, Hamada R, Miura K, et al. Bardet-Biedl syndrome in two unrelated patients with identical compound heterozygous SCLT1 mutations. *CEN Case Rep*. 2020;9(3):260-265. doi:10.1007/s13730-020-00472-y.
52. Wang C, Li Y, Shi L, et al. Mutations in SLC20A2 link familial idiopathic basal ganglia calcification with phosphate homeostasis. *Nat Genet*. 2012;44(3):254-256. Published 2012 Feb 12. doi:10.1038/ng.1077
53. Karczewski KJ, Francioli LC, Tiao G, et al. The mutational constraint spectrum quantified from variation in 141,456 humans. *Nature*. 2020;581(7809):434-443. doi:10.1038/s41586-020-2308-7
54. Fokkema IFAC, Kroon M, López Hernández JA, et al. The LOVD3 platform: efficient genome-wide sharing of genetic variants. *Eur J Hum Genet*. 2021;29(12):1796-1803. doi:10.1038/s41431-021-00959-x
55. Landrum MJ, Lee JM, Riley GR, et al. ClinVar: public archive of relationships among sequence variation and human phenotype. *Nucleic Acids Res*. 2014;42(Database issue):D980-D985. doi:10.1093/nar/gkt1113
56. Yoshida S, Yoshida K. New insights into the roles for DYRK family in mammalian development and congenital diseases. *Genes & Diseases*. 2022;10(3):758. doi:10.1016/j.gendis.2021.12.004
57. Dolgachev VA, Goldberg R, Suresh MV, et al. Electroporation-mediated delivery of the FER gene in the resolution of trauma-related fatal pneumonia. *Gene Ther*. 2016;23(11):785-796. doi:10.1038/gt.2016.58
58. Choi MS, Graves MJ, Matoo S, et al. The small EF-hand protein CALML4 functions as a critical myosin light chain within the intermicrovillar adhesion complex. *J Biol Chem*. 2020;295(28):9281-9296. doi:10.1074/jbc.RA120.012820
59. Ahmed ZM, Riazuddin S, Khan SN, Friedman PL, Riazuddin S, Friedman TB. USH1H, a novel locus for type I

- Usher syndrome, maps to chromosome 15q22-23. *Clin Genet.* 2009;75(1):86-91. doi:10.1111/j.1399-0004.2008.01038.x
60. Moore BA, Roux MJ, Sebbag L, et al. A Population Study of Common Ocular Abnormalities in C57BL/6N rd8 Mice. *Invest Ophthalmol Vis Sci.* 2018;59(6):2252-2261. doi:10.1167/iovs.17-23513
 61. Mattapallil MJ, Wawrousek EF, Chan CC, et al. The Rd8 mutation of the Crb1 gene is present in vendor lines of C57BL/6N mice and embryonic stem cells, and confounds ocular induced mutant phenotypes. *Invest Ophthalmol Vis Sci.* 2012;53(6):2921-2927. Published 2012 May 17. doi:10.1167/iovs.12-9662
 62. Weatherly SM, Collin GB, Charette JR, et al. Identification of Arhgef12 and Prkci as genetic modifiers of retinal dysplasia in the Crb1rd8 mouse model. *PLoS Genet.* 2022;18(6):e1009798. Published 2022 Jun 8. doi:10.1371/journal.pgen.1009798
 63. Averdunk L, Al-Thihli K, Surowy H, et al. Expanding the spectrum of EEF1D neurodevelopmental disorders: Biallelic variants in the guanine exchange domain. *Clin Genet.* 2023;103(4):484-491. doi:10.1111/cge.14290.
 64. Johnstone DL, Nguyen TTM, Zamboni J, et al. Early infantile epileptic encephalopathy due to biallelic pathogenic variants in PIGQ: Report of seven new subjects and review of the literature. *J Inherit Metab Dis.* 2020;43(6):1321-1332. doi:10.1002/jimd.12278.

Journal Pre-proof

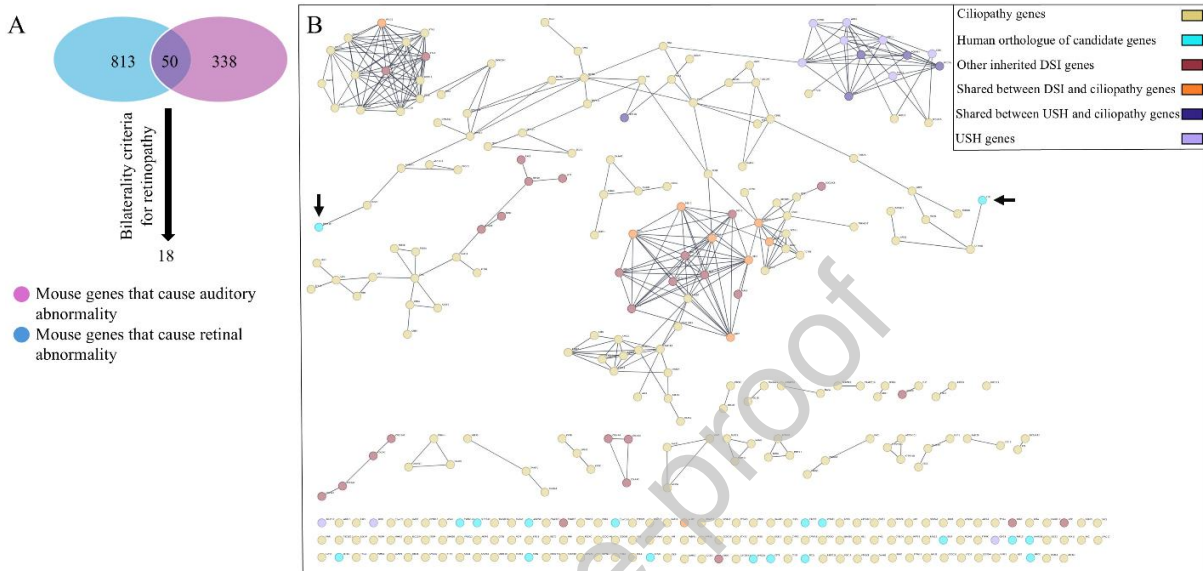


Figure 1: Identification of candidate gene list and protein interactions between proteins encoded by candidate genes and human Usher syndrome genes, other inherited dual sensory impairment syndrome genes or confirmed ciliopathy genes. (A) In the Venn diagram, IMPC genes associated with retinopathy are shown in blue and auditory abnormality causative genes are illustrated in pink. The mutual part indicates 50 genes that result in both abnormal phenotypes, concurrently. The group of 50 was further distilled to 18 genes based on our bilaterality criteria for retinopathy. (B) STRING-database was used for protein interaction analysis between proteins encoded by human orthologues of candidate genes and human USH genes, other established inherited DSI genes or confirmed ciliopathy genes. Each of these nodes indicates an encoded protein where human USH proteins, human orthologues of candidate proteins, confirmed ciliopathy proteins and other inherited DSI proteins are exhibited as nodes colored in lilac, blue, yellow and red, respectively. Shared proteins encoded by the list of other inherited DSI genes and confirmed ciliopathy genes are shown in orange. Similarly, mutual proteins among human USH proteins and ciliopathy proteins are exhibited in purple nodes. Any interaction between the protein product of each gene with a confidence of greater than or equal to 0.9 is illustrated as a line. No associations between proteins encoded by human orthologues of candidate genes and human USH genes or other inherited DSI were detected. However, two separate interactions between the ciliopathy and candidate proteins (FER and DYRK1B, shown by the arrows) were detected. USH, Usher syndrome; DSI, dual sensory impairment.

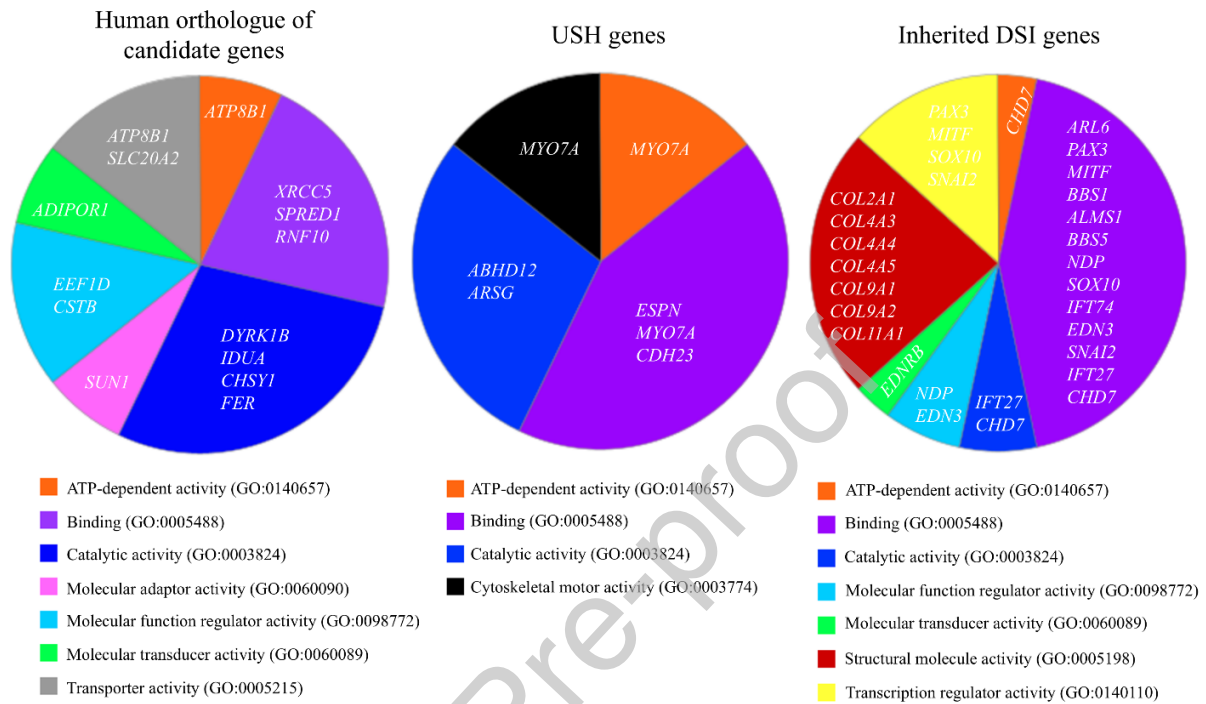


Figure 2: The molecular functions of the human orthologues of candidate genes (left), Usher syndrome genes (middle), and confirmed inherited dual sensory impairment syndrome genes (right), based on PANTHER V19.0 analysis. ATP-dependent activity, binding and catalytic activity overlap between three categories. USH, Usher syndrome; DSI, dual sensory impairment.

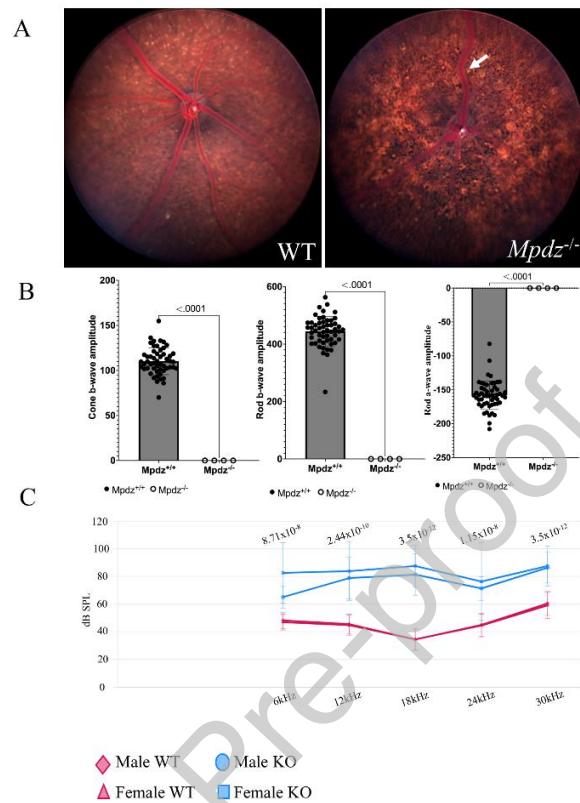


Figure 3: Fundus imaging, electroretinogram, and auditory brainstem response tests revealed retinal and hearing abnormalities in *Mpdz* knockout mice. (A) Fundus imaging of 14-week-old WT (left) and *Mpdz*^{-/-} (right) mouse revealed abnormal retina vasculature morphology in the KO mouse (indicated by an arrow). (B) ERG on 53 WT and four *Mpdz*^{-/-} mice revealed significant reduction in cone b-wave, rod b-wave, and rod a-wave amplitudes of *Mpdz*^{-/-} mice ($p < .0001$). (C) Compared to the WT mice (red lines), *Mpdz*^{-/-} mice (blue lines) showed significantly increased ABR thresholds for all tested frequencies, indicating hearing difficulties. For each tested frequency, P -value was generated by combining the ABR values of males ($n = 4$ KO, 591 WT) and females ($n = 4$ KO and 606 WT) of the same group. WT, wild-type; KO, knockout; ERG, electroretinogram; ABR, auditory brainstem response; dB SPL, decibels sound pressure level; kHz, kilohertz.

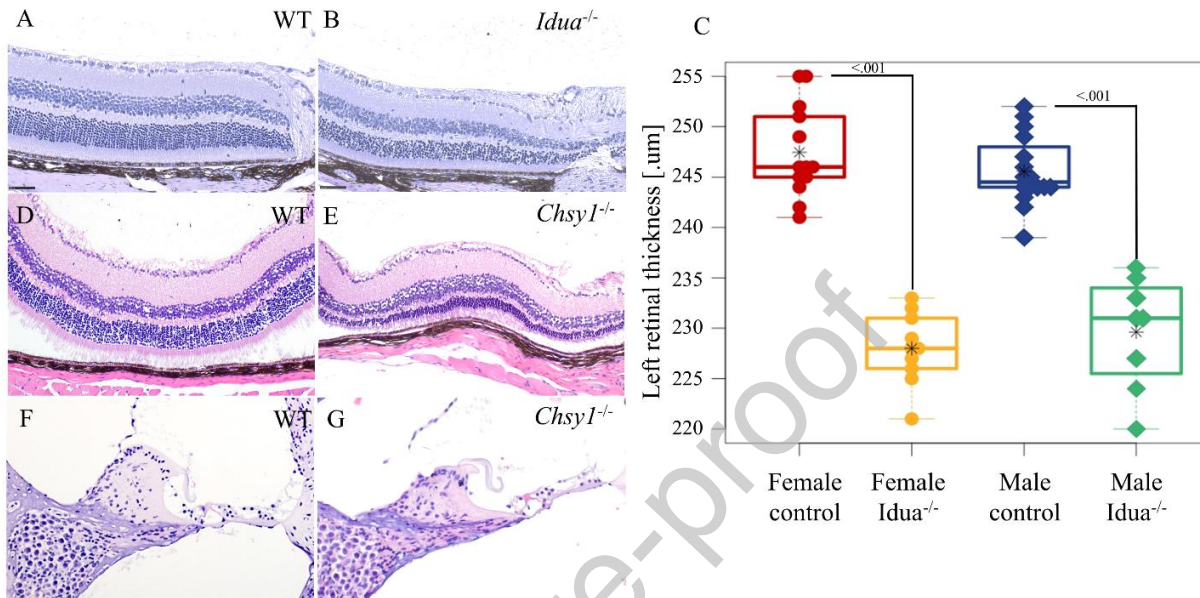


Figure 4: Morphological alterations in *Idua*^{-/-} and *Chsy1*^{-/-} mice. Comparison of representative histological images of mouse retinal tissue between 15-week-old WT (A) and *Idua*^{-/-} mice (B) showed a reduction in total retinal thickness and thinning of the outer nuclear layer in the KO mouse (hematoxylin and eosin). (C) Optical coherence tomography analysis comparing retinal thickness in 18 *Idua*^{-/-} mice (10 females and 8 males) vs 29 WT controls (13 females and 16 males) revealed a significant reduction in retinal thickness in the first group (data are shown as mean ± SEM, female $p < .001$, male $p < .001$, C). Comparison of 15-week-old WT (D) and *Chsy1*^{-/-} mice (E) demonstrated outer retinal atrophy in the KO line (hematoxylin and eosin). Examination of the organ of Corti in WT (F) and *Chsy1*^{-/-} mice (G) revealed no detectable abnormalities (hematoxylin and eosin). WT, wild-type; KO, knockout.

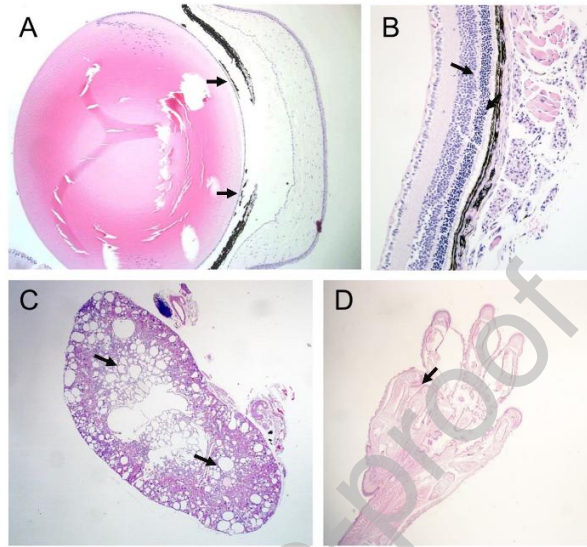


Figure 5: *Sclt1*^{-/-} mice showed eye, kidney, and skeletal abnormalities consistent with ciliopathy. (A) Eye section, showing posterior synechia of the iris to lens (indicated by arrows). (B) Retinal histology showing retinal atrophy in the outer nuclear layer and outer plexiform layer (indicated by arrows). (C) Kidney section showing multiple dilated tubules forming cystic structures, granular eosinophilic material (probably protein) and red blood cells, are evident (indicated by arrows). (D) Sections of the hind paw showing two first phalanges (indicated by an arrow) (hematoxylin and eosin).

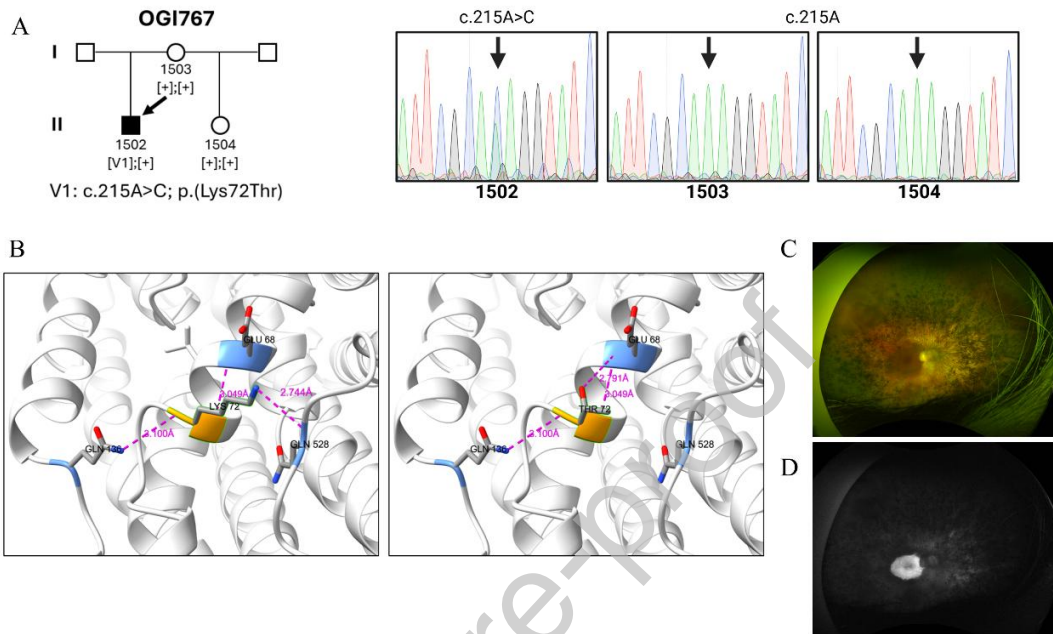


Figure 6: *SLC20A2* is a candidate gene for Usher syndrome. (A) Pedigree of an Usher syndrome type 1 family in which the affected proband (1502) harbors the missense variant p.(Lys72Thr) in *SLC20A2*, which is not present in the unaffected mother (1503) and maternal half-sister (1504); (B) ChimeraX-generated model of native (left) and mutated (right) *SLC20A2* protein. The p.Lys72Thr is predicted to alter the hydrogen bonds (indicated by purple dotted lines) with residues of Glutamic acid (Glu) and Glutamine (Gln) at positions 68 and 528, respectively; (C) Fundus and (D) fundus autofluorescence pictures of the affected proband showing findings typical of retinitis pigmentosa.

Inherited dual sensory impairment syndromes	Related candidate genes
Bardet-Biedl syndrome	<i>Atp8b1, Fer, Idua, Pigq, Rnf10, Slc20a2, Spred1, Sun1, Tmem145, Xrcc5</i>
Alstrom disease	<i>Atp8b1, Fer, Pigq, Rnf10, Spred1, Sun1, Xrcc5</i>
Tietz albinism deafness syndrome	none found
Waardenburg syndrome	<i>Chsy1</i>
Kearns-Sayre syndrome	<i>Adipor1, Ankrd11, Atp8b1, Dyrk1b, Fer, Mpdz, Pigq, Rnf10, Spred1, Sun1, Tmem145, Xrcc5</i>
Maternally inherited diabetes and deafness	<i>Adipor1, Atp8b1, Fer, Mpdz, Rnf10, Spred1, Sun1, Tmem145, Xrcc5</i>

Stickler syndrome	<i>Atp8b1, Fer, Pigq, Rnf10, Spred1, Xrcc5</i>
Norrie disease	<i>Ankrd11, Atp8b1, Dyrk1b, Pigq, Rnf10, Spred1, Sun1, Tmem145</i>
Charge syndrome	<i>Adipor1, Ankrd11, Atp8b1, Cstb, Fer, Idua, Mpdz, Pigq, Rnf10, Slc20a2, Spred1, Sun1, Xrcc5</i>
Alport syndrome	AA986860, <i>Atp8b1, Eef1d, Fer, Rnf10, Spred1, Tmem145, Xrcc5</i>

Table 1: Candidate genes whose mouse lines are phenotypically similar to non-Usher inherited dual sensory impairment syndromes. Mutant mouse lines of the candidate genes associated with these syndromes showed abnormal phenotypes in at least two different physiological systems similar to the systems affected by the syndrome, in addition to the retina and hearing phenotype.

Mouse orthologue of Usher syndrome genes	IMPC retina findings	IMPC inner ear findings	Literature retina, PMID	Literature retina findings	Literature inner ear, PMID	Literature inner ear findings
<i>Abhd12</i>	Not tested	Not tested	PMID: 23297193	Negative	PMID: 23297193	Positive
<i>Adgrv1</i>	Negative	Positive (abnormal ABR)	PMID: 17295842	Negative	PMID: 17295842	Positive
<i>Arsg</i>	Negative	ABR done, results not yet analyzed	PMID: 26975023	Positive	PMID: 22689975 PMID: 31927188	Negative
<i>Cdh23</i>	Eye test done, results not yet analyzed	Not tested			PMID: 21436032 PMID: 20332152	Positive
<i>Cep250</i>	Negative	Positive (abnormal ABR)	PMID: 36857066	Positive	PMID: 36857066	Positive
<i>Cep78</i>	Negative	Negative	PMID: 36206347	Positive	PMID: 36206347	Positive
<i>Clrn1</i>	Negative	Positive (abnormal ABR)	PMID: 26943149	Positive	PMID: 19680541	Positive
<i>Espn</i>	Negative	Not tested			PMID: 10975527	Positive
<i>Myo7a</i>	Negative	ABR done, results not yet analyzed	PMID: 31824252	Positive	PMID: 31824252	Positive
<i>Pcdh15</i>	Not tested	Not tested	PMID: 12939319	Negative	PMID: 18085631	Positive
<i>Pdzd7</i>	Not tested	Not tested	PMID: 24334608	Negative	PMID: 24334608	Positive
<i>Ush1c</i>	Negative	ABR done, results not yet analyzed	PMID: 20211154	Positive	PMID: 20211154	Positive

<i>Ush1g</i>	Not tested	Not tested	PMID: 37328946	Positive	PMID: 37328946	Positive
<i>Ush2a</i>	Not tested	Not tested	PMID: 17360538	Positive	PMID: 33498833	Positive
<i>Whrn</i>	Negative	Not tested	PMID: 20502675	Positive	PMID: 20502675	Positive

B

Mouse orthologue of inherited dual sensory impairment syndrome genes	IMPC retina findings	IMPC inner ear findings	Literature retina, PMID	Literature retina findings	Literature inner ear, PMID	Literature inner ear findings
<i>Alms1</i>	Negative	Negative	PMID: 16000322	Positive	PMID: 16000322	Positive
<i>Arl6</i>	Not tested	Not tested	PMID: 22139371	Positive		
<i>Bbip1</i>	Negative	ABR done, results not yet analyzed				
<i>Bbs1</i>	Negative	Negative			PMID: 16170314	Positive
<i>Bbs10</i>	Negative	Negative	PMID: 36125046	Positive		
<i>Bbs12</i>	Negative	ABR done, results not yet analyzed	PMID: 22869374	Positive		
<i>Bbs2</i>	Not tested	Not tested	PMID: 15539463	Positive		
<i>Bbs4</i>	Negative	Negative	PMID: 15173597 PMID: 29049287	Positive	PMID: 19396898	Positive
<i>Bbs5</i>	Positive (abnormal retina morphology)	Not tested	PMID: 32776140	Positive		
<i>Bbs7</i>	Negative	Negative	PMID: 23572516	Positive		
<i>Bbs9</i>	Negative	Not tested				
<i>Cep290</i>	Negative	Negative	PMID: 25859007	Positive		
<i>Cfap418</i>	Negative	Negative	PMID: 29440555 PMID: 37971880	Positive		
<i>Chd7</i>	Negative	Not tested	PMID: 26670829	Positive	PMID: 34004180	Positive
<i>Coll1a1</i>	Negative	Not tested			PMID 22567353	Positive

<i>Col2a1</i>	Negative	ABR done, results not yet analyzed	PMID: 16546167	Negative		
<i>Col4a3</i>	Negative	Negative			PMID: 9682811	Positive
<i>Col4a4</i>	Negative	Negative			PMID: 21196518	Positive
<i>Col4a5</i>	Negative	Negative				
<i>Col9a1</i>	Not tested	Not tested	PMID:16909383	Negative	PMID: 15802199	Positive
<i>Col9a2</i>	Negative	Positive (abnormal ABR)			PMID: 31161720	Positive
<i>edn3</i>	Not tested	Not tested	PMID: 8001160	Negative		
<i>Ednrb</i>	Not tested	Not tested			PMID: 21715336	Positive
<i>Ift172</i>	Positive (abnormal retina blood vessel morphology)	Negative	PMID: 29659833	Positive		
Mouse orthologue of inherited dual sensory impairment syndrome genes	IMPC retina findings	IMPC inner ear findings	Literature retina, PMID	Literature retina findings	Literature inner ear, PMID	Literature inner ear findings
<i>Ift27</i>	Not tested	Not tested			PMID: 25605782	Positive
<i>Ift74</i>	Negative	Negative				
<i>Lztf11</i>	Not tested	Not tested	PMID: 27312011	Positive		
<i>Mitf</i>	Not tested	Not tested	PMID: 31659211	Positive	PMID: 31659211	Positive
<i>Mkks</i>	Not tested	Not tested	PMID: 22446187	Positive	PMID: 22446187	Positive
<i>Mks1</i>	Negative	Not tested				
<i>mt-T11</i>						
<i>Ndp</i>	Not tested	Not tested	PMID: 12040033 PMID: 8789439	Positive	PMID: 34544869	Positive
<i>Pax3</i>	Not tested	Not tested			PMID: 38278860	Positive
<i>Sdccag8</i>	Not tested	Not tested				
<i>Snai2</i>	Negative	Negative				
<i>Sox10</i>	Not tested	Not tested				
<i>Trim32</i>	Not tested	Not tested				
<i>Ttc8</i>	Not tested	Not tested	PMID: 29049287	Positive	PMID: 25605782	Positive
<i>Wdpcp</i>	Not tested	Not tested				

Table 2: Comparison of IMPC phenotyping results and independent lab findings based on our literature search regarding mutant mice of mouse orthologues of human Usher genes and non-Usher inherited dual sensory impairment syndrome genes. The results showed that the longitudinal studies conducted by independent labs may be

more successful in identifying abnormal phenotypes of mutant mouse lines of USH genes (A) and other inherited DSI syndrome genes (B) compared to the high-throughput ‘snapshot-in-time’ screening done by IMPC centers. IMPC, international mouse phenotyping consortium; ABR, abnormal auditory brainstem response.

Phenotype in knockout mouse models	IMPC knockout mouse lines	Peer-reviewed articles of knockout mouse lines
Retinal abnormality	USH: 0/9	USH: 7/8
	Other inherited DSI: 2/22	Other inherited DSI: 10/11
Hearing abnormality	USH: 3/4	USH: 4/4
	Other inherited DSI: 1/14	Other inherited DSI: 6/6
Mouse models with both phenotypes evaluated	USH: 0/4	USH: 3/4
	Other inherited DSI: 0/14	Other inherited DSI: 2/2

Table 3: Comparing the head-to-head concordance of retinal and auditory phenotypes between similar mutant mouse lines from the IMPC and peer-reviewed articles from independent researchers. Of the 15 USH genes in humans, each has a mouse orthologue. Of these 15 mouse genes, the IMPC has phenotyped the retina of nine and the hearing ability of four KO/HET lines. Independent labs in the peer-reviewed literature evaluated reported retinal abnormalities in eight of the nine genes, and hearing abnormalities in all four lines. The IMPC phenotyping process found 0/9 or 3/4 of the mouse orthologs of human USH genes have retinopathy or hearing impairment, respectively. Of these four lines studied by independent labs, all had a definitive hearing impairment and of the eight KO lines that underwent ophthalmological assessment, seven exhibited retinal abnormality. Furthermore, independent studies showed that among four IMPC KO lines, which were phenotyped regarding both retina and inner ear, three exhibited abnormalities, concurrently. However, these abnormalities were not reported by IMPC (0/4). Similarly, of the 39 other DSI genes in humans, all have a mouse orthologue. Of these 39 genes, the IMPC had phenotyped the retina of 22 and hearing ability of 14 KO/HET/hemizygous lines. The IMPC data showed that 2/22 (9.1%, *Bbs5* and *Ift172*) of these models had retinopathy. In addition, 1/14 (7.1%, *Col9a2*) of the mutant lines have hearing impairment. Only 11 of these 22 genes, and six of these 14 genes with IMPC mutants have mouse lines evaluated by independent labs in the peer-reviewed literature for head-to-head comparison regarding retina and inner ear, respectively. In the published literature, ten lines documented evidence of retinopathy and all six lines had abnormalities in the inner ear. Additionally, out of 14 IMPC mutant lines, which were studied for both retinopathy and inner ear abnormality, only two were studied regarding both retina and inner ear by the independent labs. Both lines (*Bbs4* and *Alms1*) showed abnormal phenotypes simultaneously. While IMPC phenotyping is comprehensive for all systems, some of these lines generated by others were not evaluated for all systems. Mutant mouse models of bona fide human USH/DSI genes relatively faithfully recapitulate both hearing and retinal abnormalities seen in people, but longitudinal screening may be required to identify them, while high-throughput snapshot screening may miss subtle defects, especially on the *rd8* background. IMPC, international mouse phenotyping consortium; USH, Usher syndrome; KO, knockout; Het, heterozygous; DSI, dual sensory impairment.

Mutual signaling pathways between candidate genes and Usher syndrome genes		Mutual signaling pathways between candidate and other inherited dual sensory impairment syndrome genes	
KEGG	Reactome	KEGG	Reactome

Lysosome	Metabolism of proteins Signal Transduction Post-translational protein modification Cell Cycle Metabolism	Adherens junction Cytoskeleton in muscle cells	Metabolism of proteins Signal Transduction Post-translational protein modification Cell Cycle Immune System Innate Immune System Neutrophil degranulation Signaling by Receptor Tyrosine Kinases Cytosolic sensors of pathogen-associated DNA
----------	--	---	---

Table 4: Shared signaling pathways of candidate genes with Usher syndrome genes and other inherited dual sensory impairment syndrome genes based on DAVID v2025_1 database.